

DEVELOPMENT OF SELF-ACTING SEALS FOR HELICOPTER ENGINES

by

Peter Lynwander

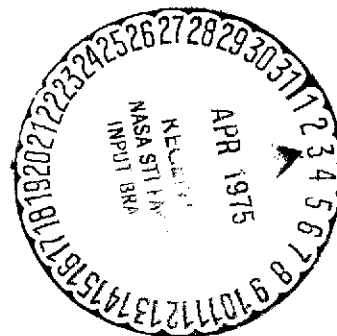
AVCO LYCOMING DIVISION
550 South Main Street
Stratford, Connecticut 06497

prepared for

NATIONAL AERONAUTICS AND SPACE ADMINISTRATION

CONTRACT NAS 3-16823

NASA Lewis Research Center
Cleveland, Ohio



N75-19243

Unclas
G3/07 13373

(NASA-CR-134739) DEVELOPMENT OF SELF-ACTING
SEALS FOR HELICOPTER ENGINES (AVCO LYCOMING
DIV.) 72 p HC \$4.25
CSCL 11A

1. Report No. NASA CR 134739		2. Government Accession No.		3. Recipient's Catalog No.	
4. Title and Subtitle DEVELOPMENT OF SELF-ACTING SEALS FOR HELICOPTER ENGINES				5. Report Date October 1974	
				6. Performing Organization Code	
7. Author(s) P. Lynwander				8. Performing Organization Report No. LYC 74-55	
9. Performing Organization Name and Address Avco Lycoming Division 550 South Main Street Stratford, Connecticut 06497				10. Work Unit No.	
				11. Contract or Grant No. NAS 3-16823	
				13. Type of Report and Period Covered Contractor Report	
12. Sponsoring Agency Name and Address National Aeronautics and Space Administration Washington, D.C. 20546				14. Sponsoring Agency Code	
15. Supplementary Notes Project Manager, Lawrence P. Ludwig, Fluid Systems Components Division NASA Lewis Research Center, Cleveland, Ohio					
16. Abstract An experimental evaluation of a NASA-designed self-acting face seal for use in advanced gas turbine main shaft positions was conducted. The seal incorporated Rayleigh step pads (self-acting geometry) for lift augmentation. Satisfactory performance of the gas film seal was demonstrated in a 500-hour endurance test at speeds to 183 m/s (600 ft/sec, 54,000 rpm) and air pressure differential of 137 N/cm ² (198.7 psi). Carbon wear was minor. Tests were also conducted with seal seat runout greater than that expected in engine operation and in a severe sand and dust environment. Seal operation was satisfactory in both these detrimental modes of operation.					
17. Key Words (Suggested by Author(s)) Self-acting face seal Lift pads Seal seat runout Sand and dust			18. Distribution Statement Unclassified — Unlimited		
19. Security Classif. (of this report) Unclassified		20. Security Classif. (of this page) Unclassified		21. No. of Pages 71	
				22. Price*	

FOREWORD

This program was funded by the U. S. Army Air Mobility Research and Development Laboratory. Program management was by the Lewis Research Center of the National Aeronautics and Space Administration under Contract NAS 3-16823. The period of performance was September 1972 to August 1974.

Technical direction was provided by the NASA project manager, Mr. Lawrence P. Ludwig of the Fluid Systems Components Division. Mr. Leonard W. Schopen, NASA Lewis Research Center, was the Contracting Officer.

The Avco Lycoming test program was carried out by Mr. Harry Thornton.

PRECEDING PAGE BLANK NOT FILMED

TABLE OF CONTENTS

	<u>Page</u>
FOREWORD	iii
LIST OF ILLUSTRATIONS	vi
LIST OF TABLES	ix
SUMMARY	1
INTRODUCTION	2
SELF-ACTING FACE SEAL DESIGN	4
TEST VEHICLE	7
EXPERIMENTAL EVALUATION AND DISCUSSION OF TEST RESULTS	12
Endurance Testing	12
Temperature Test Runs	30
Effects of Axial Runout	35
Sand and Dust Evaluation	38
CONCLUSIONS AND RECOMMENDATIONS	63
REFERENCES	64
DISTRIBUTION LIST	

PRECEDING PAGE BLANK NOT FILMED

LIST OF ILLUSTRATIONS

<u>Figure</u>	<u>Page</u>
1. Self-Acting Face Seal Design	5
2. Detail of Lift Pads	6
3. Test Vehicle and Instrumentation Plan	8
4. Test Rig Installation	9
5. Sand and Dust Test Setup	11
6. Air and Seal Temperatures During 500-Hour Endurance Test	14
7. Trace of Forward and Aft Seal Carbon Ring Sealing Faces Before 500-Hour Endurance Test - Trace Taken Radially Across a Self-Acting Lift Pad	16
8. Trace of Forward and Aft Seal Carbon Ring Sealing Faces After 500-Hour Endurance Test - Trace Taken Radially Across a Self-Acting Lift Pad	18
9. Forward Self-Acting Face Seal Seat Trace of Roughness and Waviness After Second 100-Hour Endurance Test - Trace Taken in a Radial Direction on the Seat Face Across the Running Track	20
10. Aft Self-Acting Face Seal Seat Trace of Roughness and Waviness Before 500-Hour Endurance Test - Trace Taken in a Radial Direction on the Seat Face Across the Running Track	21
11. Forward Self-Acting Face Seal Seat Trace of Roughness and Waviness After 500-Hour Endurance Test - Trace Taken in a Radial Direction on the Face Seat Across the Running Track	22
12. Aft Seal Self-Acting Face Seal Seat Trace of Roughness and Waviness After 500-Hour Endurance Test - Trace Taken in a Radial Direction on the Face Seat Across the Running Track	23

LIST OF ILLUSTRATIONS (Continued)

<u>Figure</u>	<u>Page</u>
13. Cracked Oil Dam and Heat Shield, Oil Side	24
14. Cracked Oil Dam and Heat Shield, Seat Side	25
15. Oil Dam and Heat Shield, Crack Surface	26
16. Stress Analysis of the Oil Dam	27
17. Trace of Forward Carbon Flatness After 500-Hour Endurance Test.....	28
18. Trace of Aft Carbon Flatness After 500-Hour Endurance Test	29
19. Condition of Forward Carbon and Seat After 500- Hour Endurance Test	31
20. Condition of Aft Carbon and Seat After 500-Hour Endurance Test	32
21. Condition of Forward Carbon Ring and Seat After the Temperature Test	34
22. Seat Face Axial Runout in the Free State	37
23. Airflow Through Two Seals Versus Pressure Differen- tial at 145 m/s (475 ft/sec) - Seat Face Axial Runout Testing	40
24. Static Calibrations Prior to Runout Testing	41
25. Sand and Dust Test Windback Configurations	45
26. Trace of Aft Seal Lift Pad Before and After Sand and Dust Test I	47
27. Aft Seal Seat After Sand and Dust Test I	48

LIST OF ILLUSTRATIONS (Continued)

<u>Figure</u>		<u>Page</u>
28.	Trace of Aft Seal Seat Roughness Before and After Sand and Dust Test I - Trace Taken in a Radial Direction on the Seat Face Across the Running Track	49
29.	Trace of Aft Seal Seat Waviness Before and After Sand and Dust Test I - Trace Taken in a Radial Direction on the Seat Face Across the Running Track	50
30.	Aft Seal After Sand and Dust Test IV Viewed From the Air Side	55
31.	Aft Seal After Sand and Dust Test IV Viewed From the Oil Side.....	56
32.	Forward Seal After Sand and Dust Test IV	57
33.	Seal Seats and Aft Rotating Windback After Sand and Dust Test IV	58
34.	Forward Seal Seat Surface Texture After Sand and Dust Test IV - Trace Taken in a Radial Direction on the Seat Face Across the Running Track	59
35.	Aft Seal Seat Surface Texture After Sand and Dust Test IV - Trace Taken in a Radial Direction on the Seat Face Across the Running Track	60
36.	Typical Lift Pad Traces of Forward and Aft Seal After Sand and Dust Test IV	61

LIST OF TABLES

<u>Table</u>		<u>Page</u>
I	Instrumentation Plan	10
II	500-Hour Endurance Test Results	13
III	Lift Pad Recess Depths During 500-Hour Endurance Test	17
IV	Seal Seat Surface Texture Before and After 500-Hour Endurance Test	19
V	Temperature Test Results	33
VI	Seat Face Axial Runout Evaluation - Baseline Test	36
VII	Seat Face Axial Runout Evaluation	39
VIII	"Arizona Road Dust" Dirt Particle Size Distribution	42
IX	Sand and Dust Baseline Test	43
X	Sand and Dust Test I	46
XI	Sand and Dust Test II	51
XII	Sand and Dust Test III	53
XIII	Sand and Dust Test IV	54

SUMMARY

An experimental evaluation of a NASA-designed self-acting face seal intended for use in advanced gas turbine engine main shaft positions was conducted. The self-acting face seal incorporates Rayleigh step lift pads on the carbon sealing face which provide a self-acting force to separate the sealing surfaces during operation.

In a previous program (Reference 1), self-acting and conventional gas turbine main shaft seals were evaluated, and the self-acting face seal showed the best potential for successful operation at advanced engine conditions.

The subject program was a follow-on to the initial testing and had two objectives:

1. Subject the seal to 500-hours of endurance testing at severe operating conditions.
2. Evaluate seal operation in two detrimental regimes of operation; excessive seal seat runout and a sand and dust environment.

High rotating speed and air pressure capability of the self-acting face seal were demonstrated in a 500-hour endurance test that was successfully completed. Test conditions were sliding speed to 183 m/s (600 ft/sec, 54,600 rpm), 137 N/cm^2 (198.7 psi) air pressure differential and air temperature to 381K (225°F). Carbon wear was minor.

Tests were conducted with seal seat axial runout of 0.051mm (0.002 in.) - twice the maximum level normally allowed. Operating conditions were speeds to 145 m/s (475 ft/sec, 43,000 rpm) and air pressure differential to 119 N/cm^2 (173 psi). Inspection following 10 hours of operation revealed no carbon wear or seal component distress.

Tolerance to a severe sand and dust environment was demonstrated in a series of tests introducing "Arizona Road Dust" in the rig air supply. Ten hours of stable operation were successfully completed with .03 kg/hr (1 oz/hr) of contaminant at a sliding speed of 122 m/s (400 ft/sec, 36,400 rpm) and air pressure differential of 106 N/cm^2 (154 psi).

INTRODUCTION

Main shaft seals are becoming increasingly critical in advanced gas turbine engines for helicopters. As shaft speed, air temperatures, and air pressures increase, engine size decreases, leaving less envelope to accomplish the sealing function.

The purpose of this program was to develop gas turbine main shaft seals capable of operating at conditions more severe than those experienced in current engines.

Advanced Avco Lycoming engines in the 1.36 to 4.54 kg/s (3 to 10 lb/sec) class incorporate main shaft seals that operate with surface speeds to 137 m/s (450 ft/sec), air pressure differential to 55 N/cm² (80 psi), and air temperatures to 810 K (1000°F). Positive-contact carbon seals are used. In future high-performance engines, seal operating conditions will be more severe and existing positive-contact seal configurations may not be adequate. At high speeds and pressures, positive-contact carbon seals have a tendency to wear, generate heat, and coke up.

An alternative to positive-contact seals are labyrinth seals. Because of their noncontacting feature, labyrinth seals offer infinite life; however, at high air pressures and temperatures, simple labyrinths will not suffice, and complicated multistage labyrinths must be used. These latter seals incorporate venting and pressurization passages that are costly to produce and difficult to accommodate in small, high-performance engines. Compared with positive-contact seals, labyrinths also permit higher leakage airflows (which must be absorbed by the lubrication system) that cause a loss in engine performance.

A new design concept is the self-acting seal. The self-acting seal incorporates the best features of positive-contact seals (low leakage) and labyrinth seals (noncontacting). During operation, self-acting seals are noncontacting, the sealing surfaces being separated by a thin gas film (sealing gap) which limits gas leakage. At shutdown the seal faces are in contact. Self-acting seal designs incorporate Rayleigh step lift pads on the primary (carbon) sealing faces. These lift pads provide hydrodynamic force to separate the sealing surfaces, and the gas film is sufficiently stiff so that the primary (carbon) ring tracks the runout motions of the seat without rubbing contact.

In a previous program (Reference 1) self-acting and conventional gas turbine main shaft seals were evaluated at the following speed, air pressure, and air temperature conditions:

Seal Surface Speed to 213 m/s (700 ft/sec)
Air Pressure Differential to 131 N/cm² (189.5 psi)
Air Temperature to 645 K (675°F)

The self-acting face seal configuration showed the best potential for successful operation at advanced engine conditions.

The subject program was a follow-on to the initial testing and had two objectives:

1. Subject the self-acting face seal to 500-hours of endurance operation at severe operating conditions.
2. Evaluate the self-acting face seal configuration in two detrimental regimes of operation; excessive seal seat axial run-out and a sand and dust environment.

The experimental evaluation was carried out in a test rig that simulates engine conditions in an advanced gas producer turbine bearing location. All seal and bearing package hardware was lightweight and typical of Avco Lycoming engine design practice.

SELF-ACTING FACE SEAL DESIGN

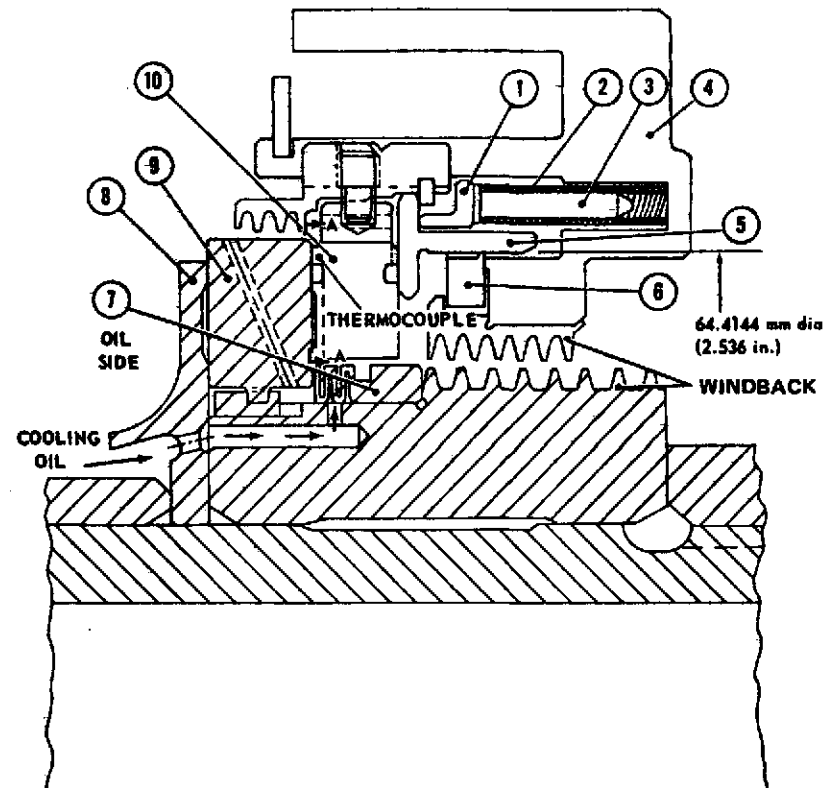
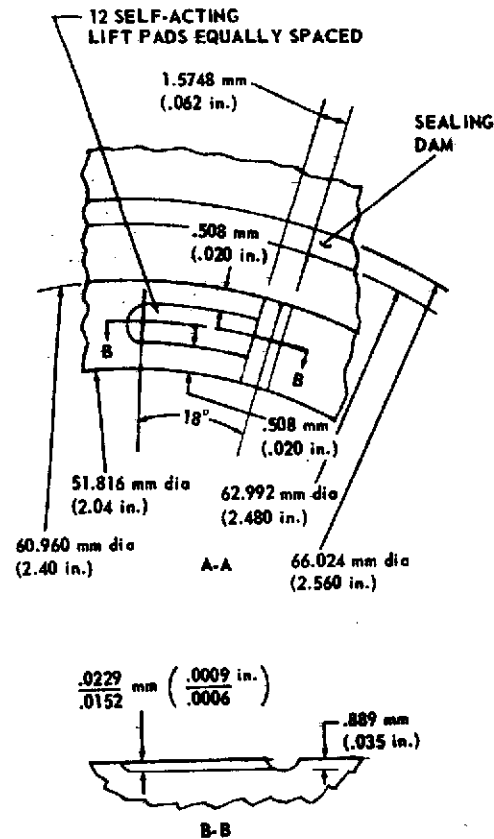
The self-acting face seal used in the test program is shown in Figure 1. It is similar to a conventional face seal with the addition of the self-acting geometry for lift augmentation.

The primary sealing interface consists of the rotating seat, which is keyed to the shaft, and the nonrotating primary ring assembly, which is free to move in an axial direction, thus accommodating axial motions due to thermal expansion. Axial springs provide the mechanical force that maintains contact between the seat and primary ring at shutdown. Spring force is 31N (7 lb). The secondary seal is a carbon piston ring, which is subjected only to the axial motion of the carrier assembly.

Great care is taken to ensure flatness of the sealing surfaces. The seat is keyed to the shaft spacer and is axially clamped by a machined bellows which minimizes distortion of the seat since the major part of the clamping force acts through the shaft spacers. The bellows also acts as a static seal between the seat and the shaft spacer. Cooling oil is passed through the seat to reduce thermal gradients, and the oil dam disc also serves as a heat shield. Windbacks are used to prevent contaminants from approaching the sealing surfaces.

In operation, the sealing faces are separated slightly, in the order of 0.00508 mm (0.0002 in.), by action of the self-acting lift geometry. This positive separation results from the balance of seal forces and the gas film stiffness of the self-acting geometry. The primary ring carbon face with the lift pads is shown in Figure 2.

To determine film thickness and air leakage in a self-acting face seal, the axial forces acting on the primary ring assembly must be determined for each operating condition. These forces comprise the self-acting lift force, the spring force, and the pneumatic forces due to the sealed pressure. Essentially the analysis requires finding the film thickness for which the opening forces balance the closing forces. When this equilibrium film thickness is known, the leakage rate can be calculated. References 2 through 8 detail the design procedure.



- | | |
|-----------------------|--------------|
| 1. SPRING PLATE | INCONEL X750 |
| 2. COMPRESSION SPRING | INCONEL X750 |
| 3. SPRING PIN | 18-8 SST |
| 4. HOUSING | INCONEL X750 |
| 5. CARRIER | INCONEL X750 |

- | | |
|----------------------------|--|
| 6. PISTON RING | HIGH-TEMPERATURE CARBON |
| 7. BELLOWS SPACER | INCONEL X750 |
| 8. OIL DAM AND HEAT SHIELD | 440 SST |
| 9. SEAT | 4340 FLAME SPRAYED WITH
LINDE LCIC (CHROME CARBIDE) |
| 10. PRIMARY RING | HIGH-TEMPERATURE
CARBON AND TZM |

Figure 1. Self-Acting Face Seal Design.

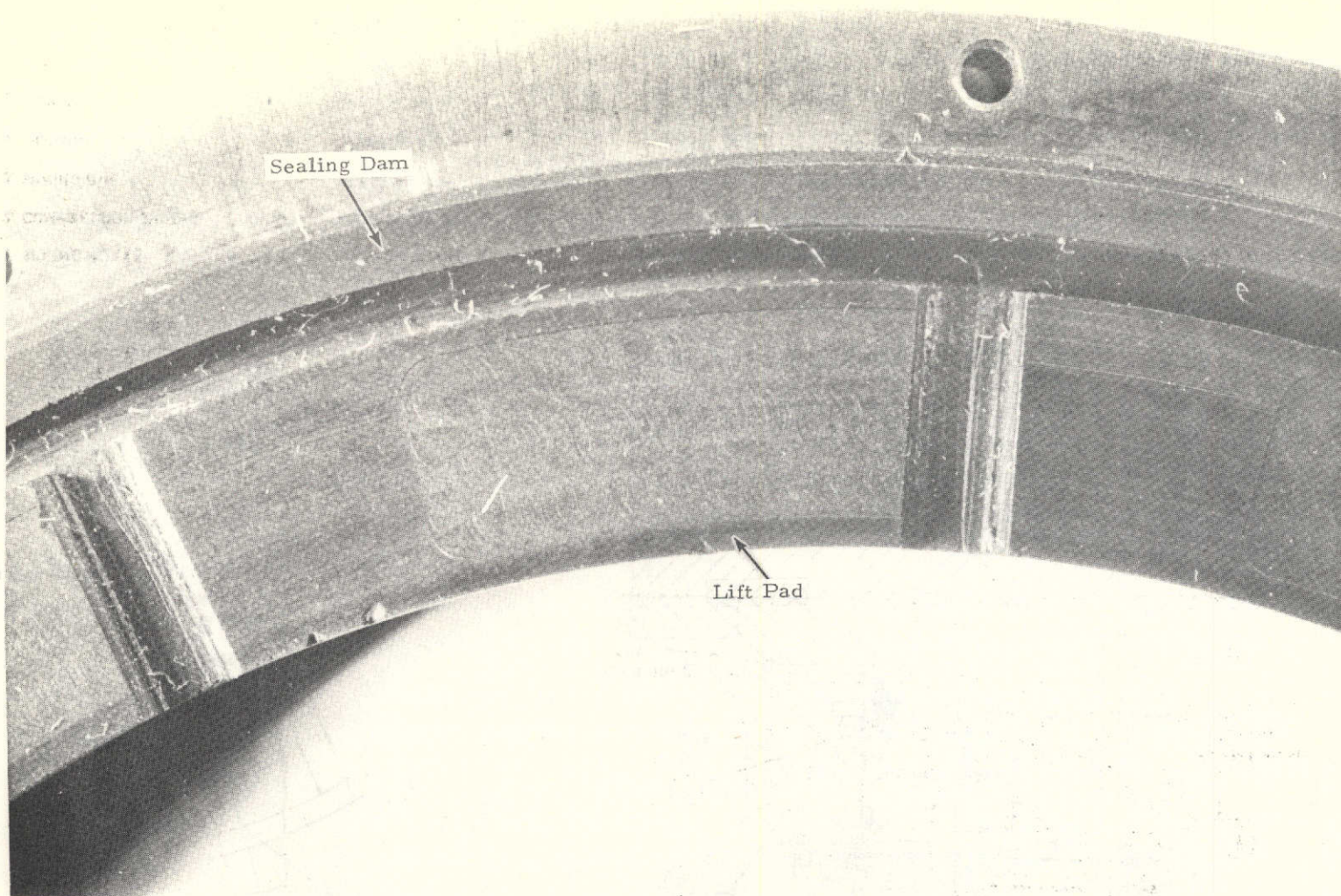


Figure 2. Detail of Lift Pads.

TEST VEHICLE

The test rig bearing compartment (Figure 3) is typical of advanced, high-speed gas turbine packages. Sealing positions are located forward and aft of the bearing, which enabled two seal samples to be tested simultaneously.

The rig prime mover is a 100-horsepower, 20,000-rpm steam turbine. Connecting the steam turbine to the rig is a 3:1 ratio speed increaser. The test installation is shown in Figure 4.

The shaft is supported by a 35-mm, split-inner-race ball bearing in the test position, and by a 25-mm, split-inner-race bearing in the support position. Both bearings are hydraulically mounted, and thrust loading is supplied by coil springs acting on the outer race of the support bearing and by pressure differentials across the loading wheel.

A single batch of MIL-L-23699 oil at 367 ± 5 K ($200 \pm 10^\circ\text{F}$) was used throughout the test program. Oil flow to the test package was 202 kg/hr (450 lb/hr). The bearing was lubricated by four 0.81 mm (0.032 in) jets and each seal seat by two 0.81 mm (0.032 in) jets.

The bearing compartment drains by gravity into a static air-oil separator. The minimum scavenge area is 93 mm^2 (0.144 in^2). Desired air pressure is introduced into the cavities adjacent to the test seals, and the air that leaks past the test seals is conveyed through a flowmeter from the air-oil separator to obtain a measure of seal performance.

Instrumentation incorporated in the test rig is listed in Table I. The location of the pertinent instrumentation is shown in Figure 3. All measurements were made with instruments using English units. These were then converted to SI units for reporting purposes.

Figure 5 illustrates the setup used in the sand and dust testing. Contaminants were placed in the sand receiver. The air-sand inlet valve was opened to allow access to the test rig aft air compartment. Then the high air pressure inlet valve was opened and the contaminants were blown into the rig.

(CIRCLED NUMBERS REFER TO TABLE I)

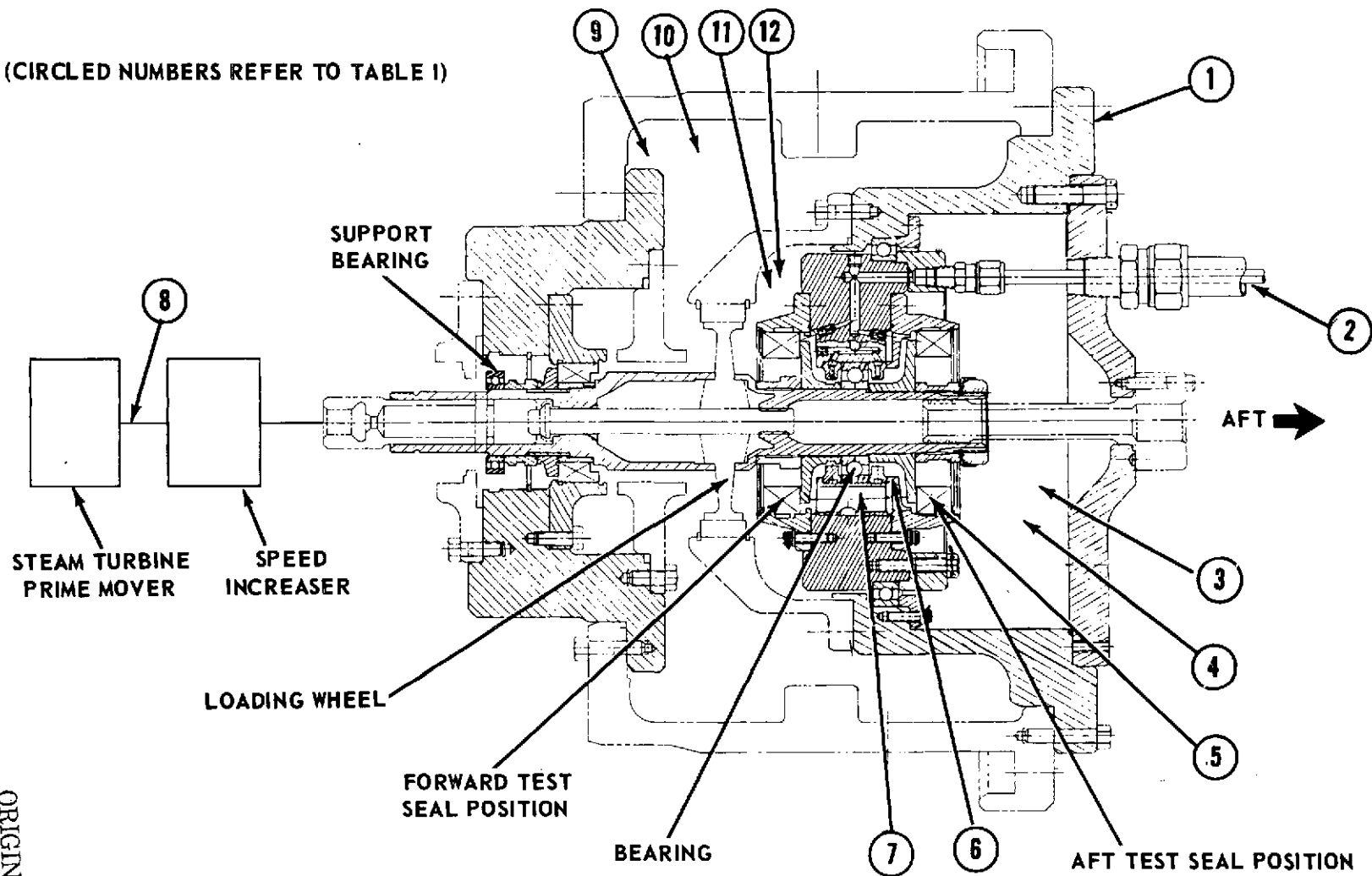


Figure 3. Test Vehicle and Instrumentation Plan.

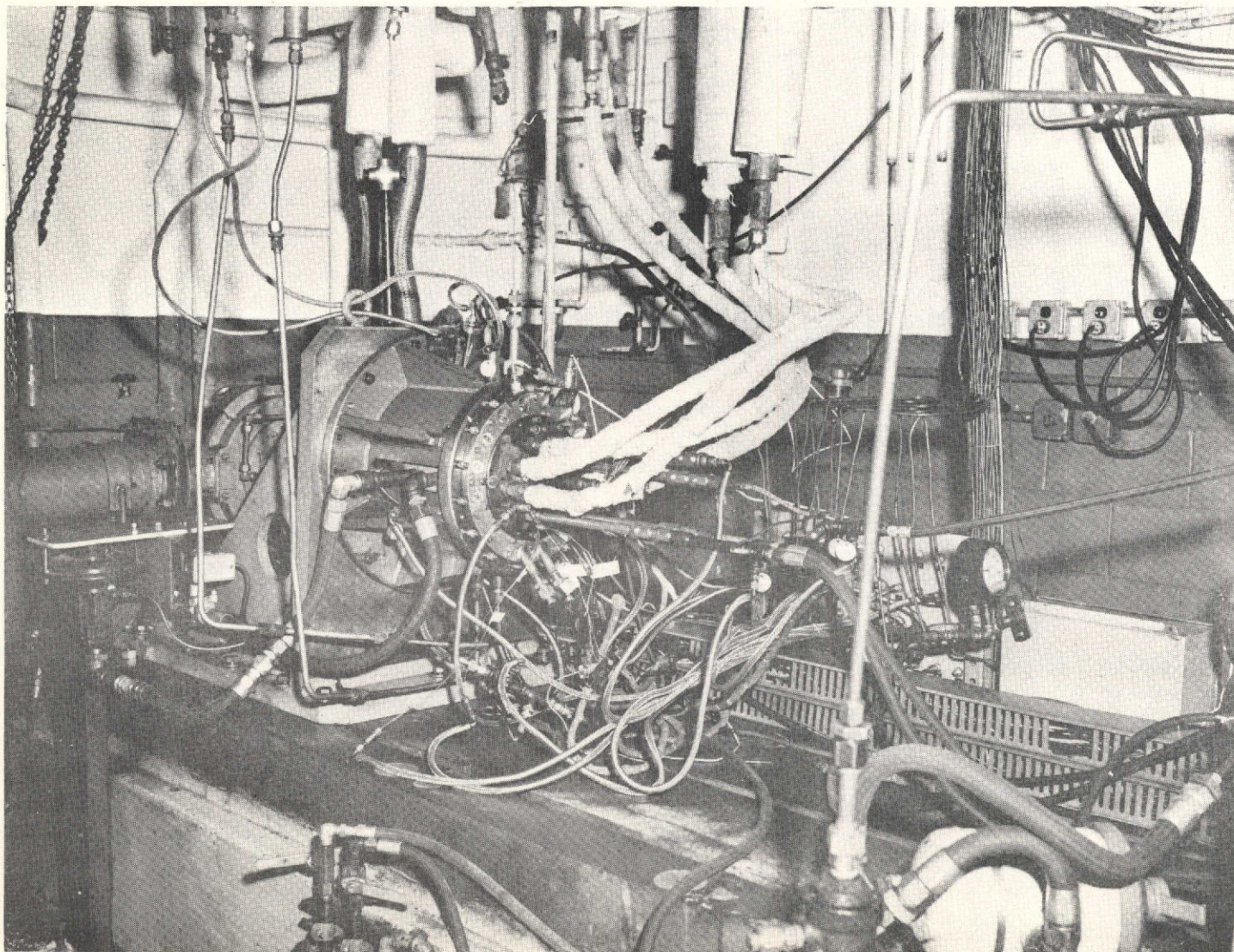


Figure 4. Test Rig Installation.

TABLE I. INSTRUMENTATION PLAN

<u>Parameter To Be Measured</u>	<u>Sensing Device</u>	<u>Location</u>	<u>Corresponding Number in Figure 3</u>
Shaft Speed	Magnetic pickup	Steam turbine shaft	8
Air Pressure	Gage	Fwd wheel cavity	9
	Gage	Fwd seal cavity	12
	Gage	Aft seal cavity	3
Air Temperature	Thermocouple	Fwd wheel cavity	10
	Thermocouple	Fwd seal cavity	11
	Thermocouple	Aft seal cavity	4
Seal Air Leakage	Glass tube rotameter	Scavenge air-oil mixture is passed through a static separator and the dry airflow is passed through the flowmeter	7
Oil Temperature	Thermocouple	Oil feed line	2
	Thermocouple	Scavenge line	7
Oil Flow	Glass tube rotameter	Oil feed line	2
Oil Pressure	Gage	Oil feed line	2
Bearing Cavity Pressure	Gage	Within bearing cavity	6
Scavenge Pressure	Gage	Scavenge line	7
Seal Temperature	Thermocouple	Seal case or carbon	5
Vibration	Velocity pickup		1
Chips	Chip detector	Scavenge line	7

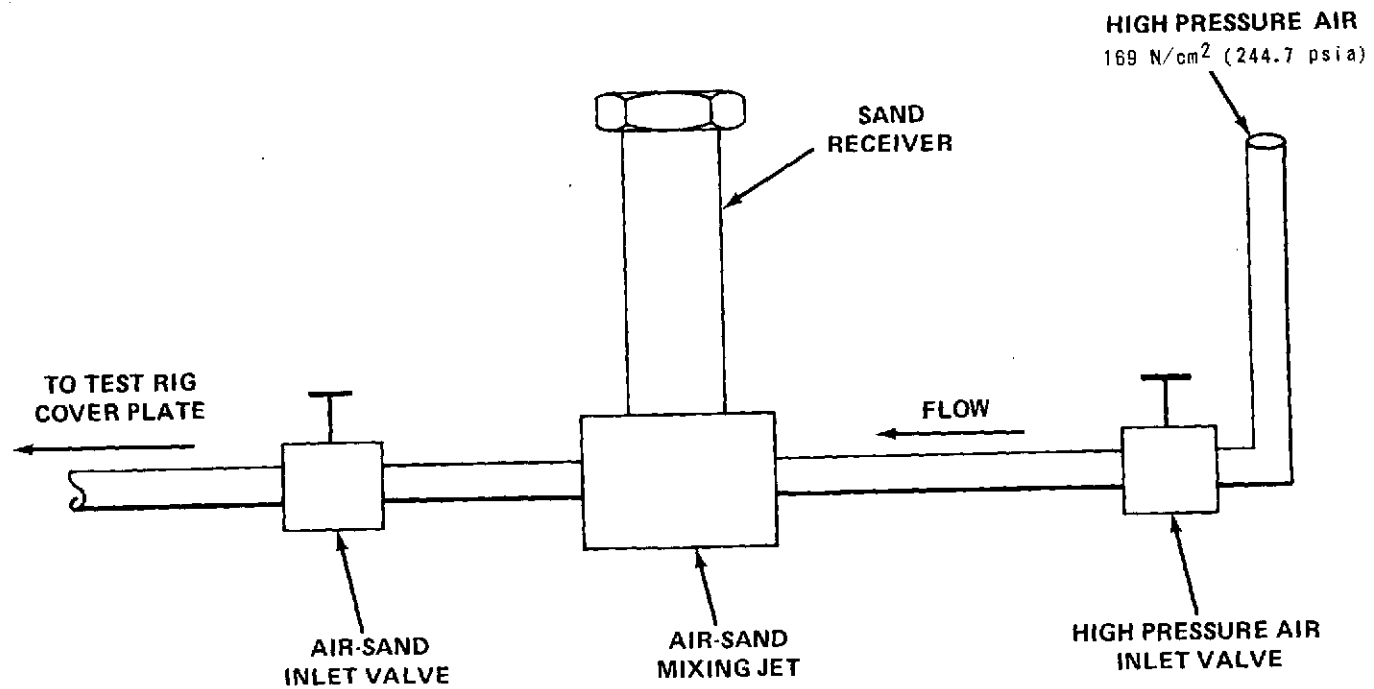


Figure 5. Sand and Dust Test Setup.

EXPERIMENTAL EVALUATION AND DISCUSSION OF TEST RESULTS Endurance Testing

A 500-hour endurance test was conducted in 100-hour increments. The test conditions were as follows:

Hours	Speed			Air Pressure Differential (max)	
	m/s	ft/sec	rpm	N/cm ²	psia
1-100	145	475	43,000	125	181
100-200	152	500	45,500	129	186.5
200-300	160	525	47,700	130	189
300-400	168	550	50,000	129	187
400-467	175	575	52,300	128	186
467-500	183	600	54,600	128	186

The same aft carbon and seat were used throughout the test. The aft seat had previously operated for 150 hours. A single forward carbon was used throughout the test. The forward carbon had previously operated for 150 hours. The forward seat was changed after the first 100 hours, and the new part operated for the final 400 hours.

Table II outlines test results for the 500-hour run. The last run was typical of the airflow that can be expected through two seals at an air pressure differential of 127 N/cm² (184 psi); approximately .007 kg/s (12 scfm or .015 lb/sec). The airflow was higher in other runs because of leakage in the rig scavenge fittings. Experience has shown that self-acting seal air leakage increases slightly with speed because the operating gap increases; however, the rig scavenge fitting air leakage obscured this phenomenon.

Air temperature did not exceed 381 K (225°F) during the 500 hours (Figure 6). At the 300-hour mark the forward seal temperature was approaching 422 K (300°F). Previous testing had shown that at seal temperatures of approximately 450 K (350°F) seal seat distortions became a problem; therefore, after the first 300 hours air temperatures were reduced by opening the rig bleeds thereby flowing more air through the rig.

TABLE II. 500 HOUR ENDURANCE TEST RESULTS -
SEALED PRESSURE 148 N/cm² abs (214.7 psia)

Hours	Maximum Airflow (two Seals)			Maximum Cavity Pressure		Maximum Fwd Seal Temp		Maximum Aft Seal Temp		No. of Stops
	(kg/s)	(scfm)	(lb/sec)	(N/cm ² abs)	(psia)	(K)	(°F)	K	°F	
1-100 ^a	.011	18.5	.024	25.3	36.7	407	272	380	225	8
100-200 ^a	.008	13.5	.017	21.8	31.7	417	290	386	234	9
200-300 ^a	.007	12.5	.016	21.5	31.2	421	298	390	242	21
300-400 ^a	.008	14.5	.018	22.5	32.7	420	296	395	251	9
400-467	.007	12.5	.016	21.2	30.7	420	296	399	258	8
467-500	.007	12.0	.015	21.2	30.7	426	306	407	272	3
a. Air leakage results includes leakage through scavenge fittings.										

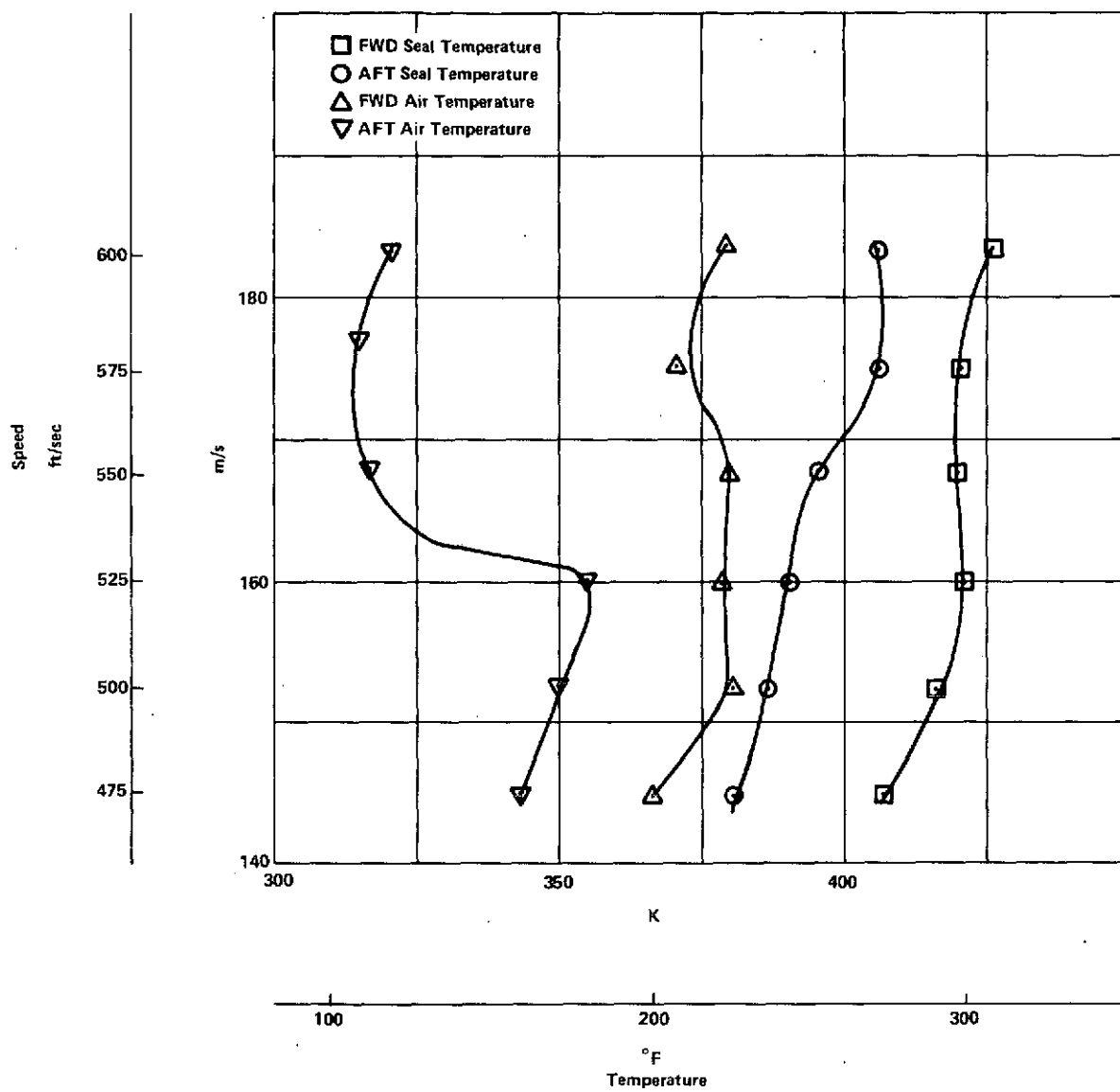


Figure 6. Air and Seal Temperatures During 500-Hour Endurance Test.

Following each phase of testing, a visual and analytical inspection was performed on the primary carbon ring and the seat. The depth of the lift pads on the primary carbon ring was measured by taking a proficorder trace radially across the face. The average total wear of the carbon faces for the 500-hour test was 0.0051 mm (0.0002 in). Traces of the primary ring sealing faces of the forward and aft seals prior to testing are shown in Figure 7. Only one pad is depicted. Traces of four of twelve pads were taken after each test. Table III lists the pad recess depths at each phase of testing. Traces of the lift pads after the 500-hour test are shown in Figure 8.

Seal seats were traces for roughness, waviness, and flatness in the unassembled state. Table IV lists these values prior to and after testing. Flatness of the assembled seats clamped in place on the shaft did not exceed 0.0015 mm (0.00007 in). Measurement charts showing seat surface texture before and after the endurance test are presented in Figures 9 through 12.

These traces were taken in a radial direction through the running track. Although some deterioration was measured, the seal seats were in acceptable condition for further operation after the 500-hour test.

Inspection following the 500-hour test revealed a problem in the forward seal. The carbon sealing face was found to be distorted, and there was a radial crack in the oil dam and heat shield.

Figures 13 and 14 show both sides of the oil dam illustrating the crack. Figure 15 is the crack surface. Metallurgical examination showed the crack to be a fibrous fracture with no trace of fatigue.

A finite element stress analysis of the oil dam at the seal operating conditions was conducted. Figure 16 presents the results of the analysis showing lines of constant stress and the point of maximum stress. The dam material is AMS 5630 heat treated to R_c 54-60 with a yield stress of $190,000 \text{ N/cm}^2$ (275,000 psi). The maximum dam stress of 128 N/cm^2 (186,381 psi) is well below this value. To date no explanation has been found for the crack.

Figure 17 presents an Indiron trace of the forward carbon sealing face showing it to be .089 mm (0.0035 in.) out of flat. In comparison Figure 18 shows the aft carbon sealing face after testing.

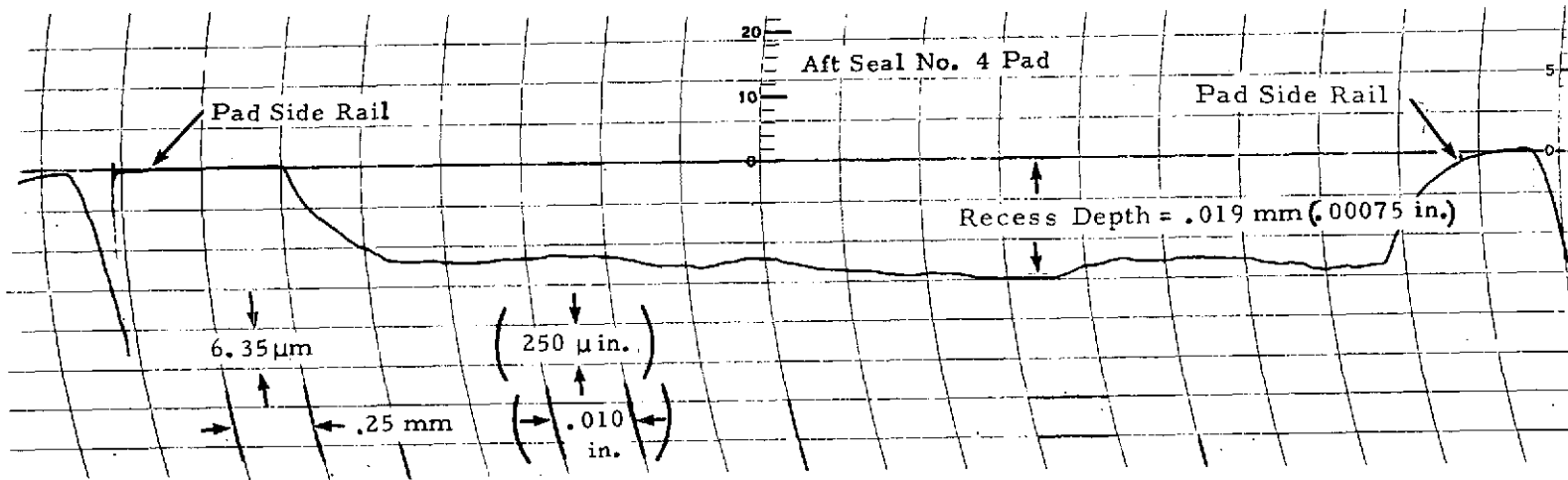
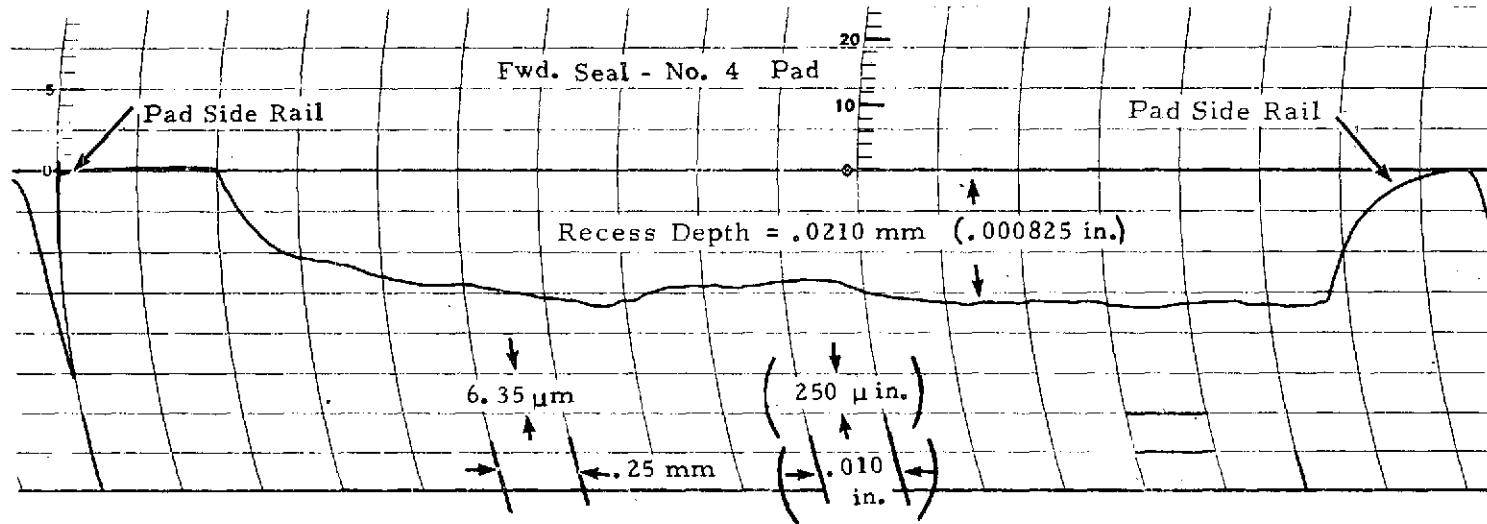


Figure 7. Trace of Forward and Aft Seal Carbon Ring Sealing Faces Before 500-Hour Endurance Test - Trace Taken Radially Across a Self-Acting Lift Pad.

TABLE III. LIFT PAD RECESS DEPTHS DURING 500-HOUR ENDURANCE TESTS

Pad	Forward Seal				Aft Seal			
	1	2	3	4	1	2	3	4
Pad Depth Prior to test								
(mm)	.018	.020	.019	.021	.017	.018	.017	.019
(in.)	.0007	.0008	.00075	.000825	.000675	.0007	.00065	.00075
100 hr								
(mm)	.018	.019	.019	.015	.017	.018	.017	.019
(in.)	.0007	.00075	.00075	.000575	.000675	.0007	.00065	.00075
200 hr								
(mm)	.017	.017	.018	.014	.017	.016	.015	.018
(in.)	.000675	.00065	.00070	.00055	.00065	.000625	.000575	.00070
300 hr								
(mm)	.017	.017	.017	.014	.015	.014	.015	.015
(in.)	.00065	.00065	.000675	.00055	.000575	.00055	.000575	.000575
400 hr								
(mm)	.017	.016	.017	.013	.015	.014	.015	.011
(in.)	.00065	.000625	.00065	.000525	.000575	.00055	.000575	.00045
500 hr								
(mm)	.016	.015	.017	.011	.013	.013	.013	.011
(in.)	.000625	.000600	.000650	.00045	.000525	.000500	.000525	.00045

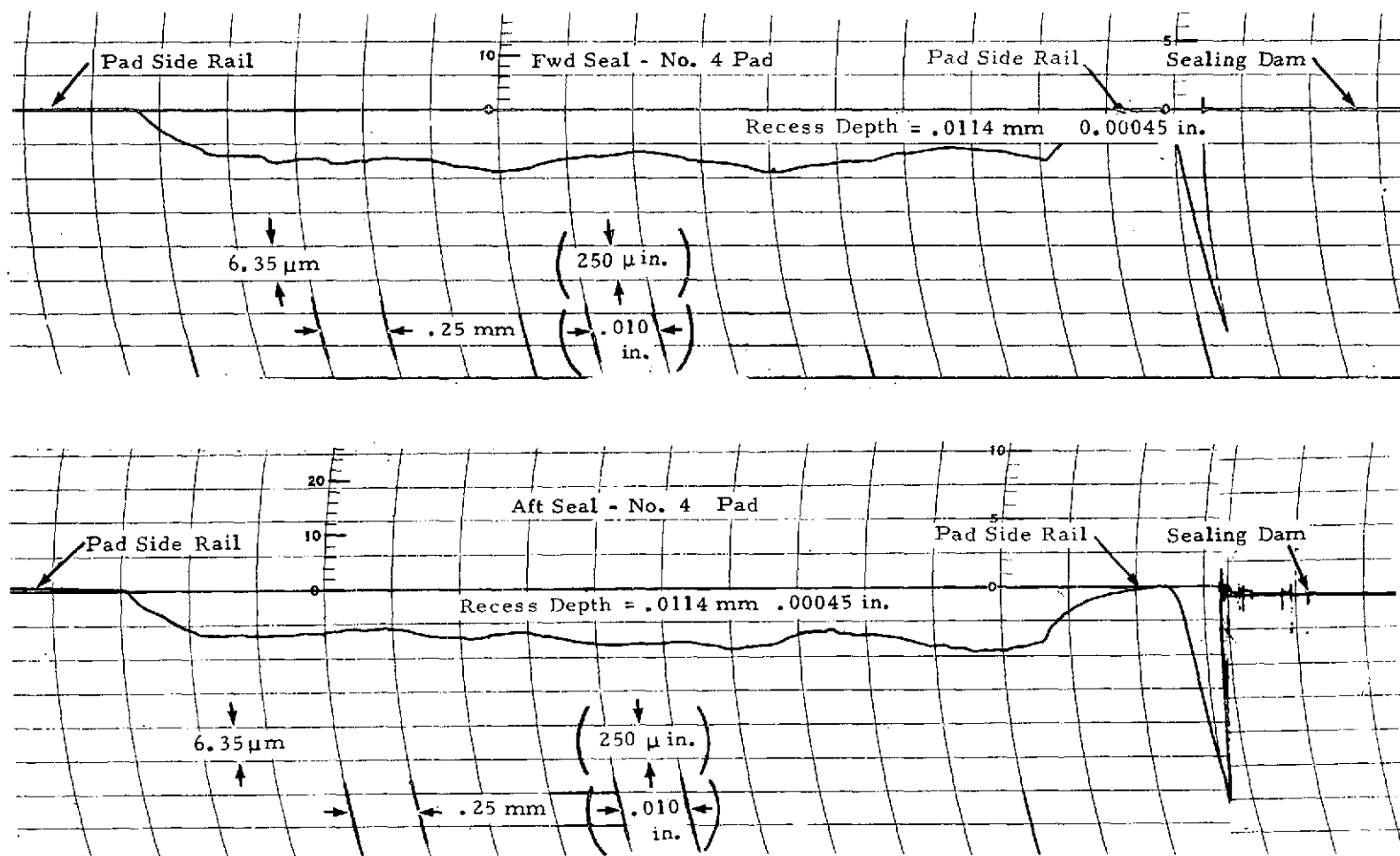


Figure 8. Trace of Forward and Aft Seal Carbon Ring Sealing Faces After 500-Hour Endurance Test - Trace Taken Radially Across a Self-Acting Lift Pad.

TABLE IV. SEAL SEAT SURFACE TEXTURE BEFORE AND
AFTER 500-HOUR ENDURANCE TEST

	Prior to Testing	After 500 Hours
<u>Fwd Seat</u>		
Flatness (μ m)	.584	.685
(in.)	.000023	.000027
Roughness (μ m)	.127	.127
(μ in. AA)	5	5
Waviness (μ m)	.457	.889
(in)	.000018	.000035
<u>Aft Seat</u>		
Flatness (μ m)	.635	.711
(in.)	.000025	.000028
Roughness (μ m)	.102	.127
(μ in. AA)	4	5
Waviness (μ m)	.228	.389
(in)	.000009	.000035

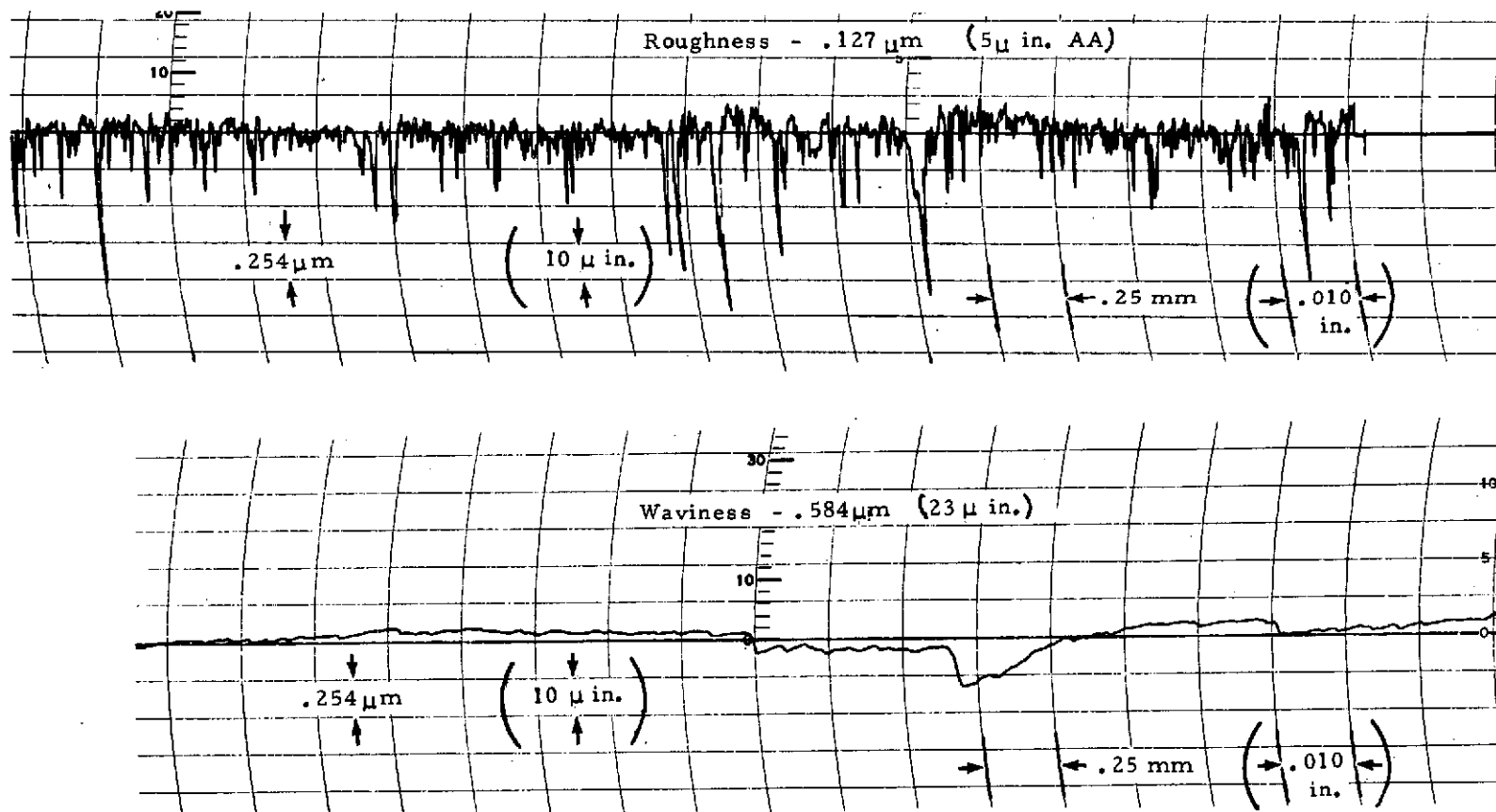


Figure 9. Forward Self-Acting Face Seal Seat Trace of Roughness and Waviness After Second 100-Hour Endurance Test - Trace Taken in a Radial Direction on the Seat Face Across the Running Track.

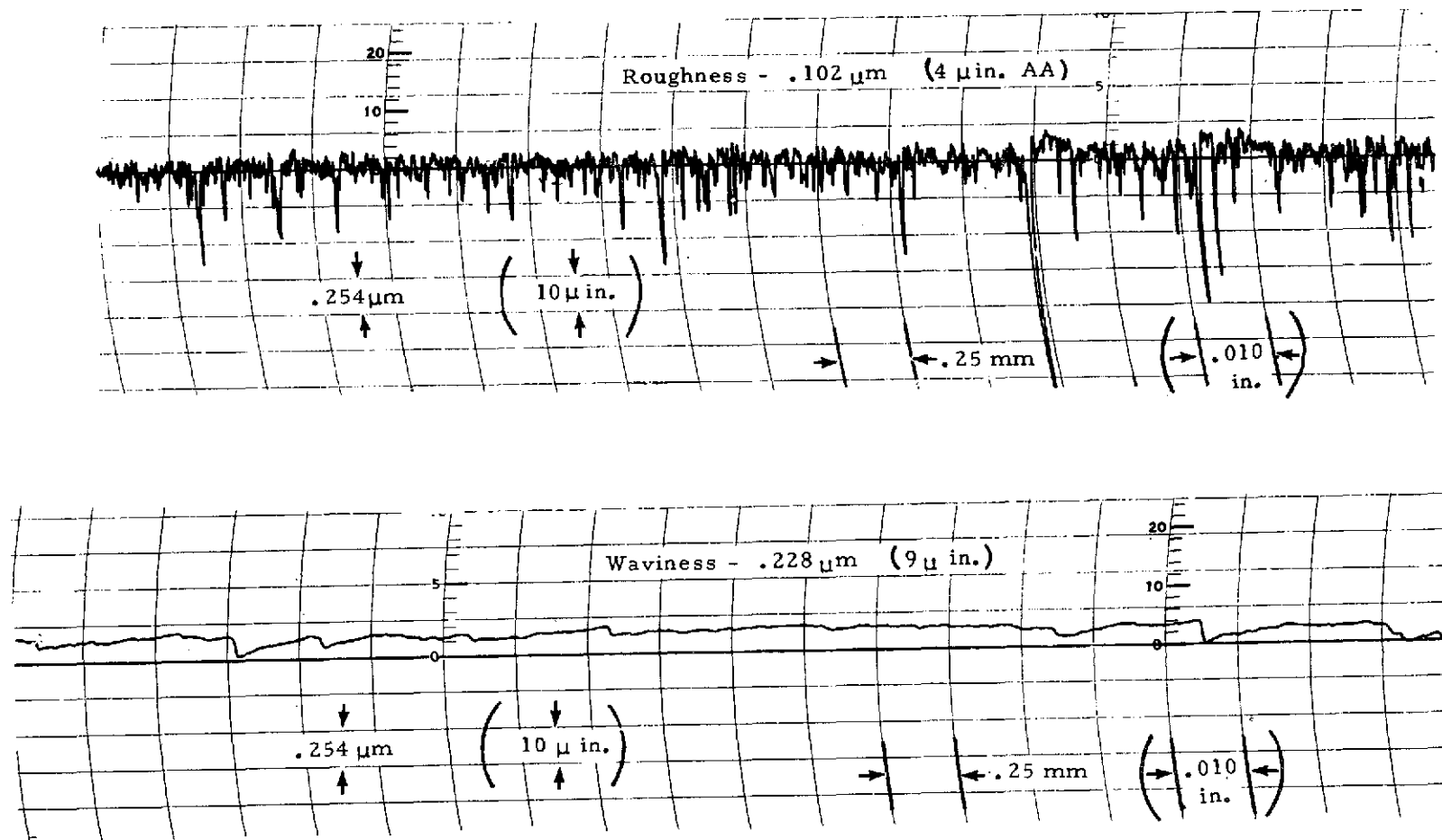


Figure 10. Aft Self-Acting Face Seal Seat Trace of Roughness and Waviness Before 500-Hour Endurance Test - Trace Taken in a Radial Direction on the Seat Face Across the Running Track.

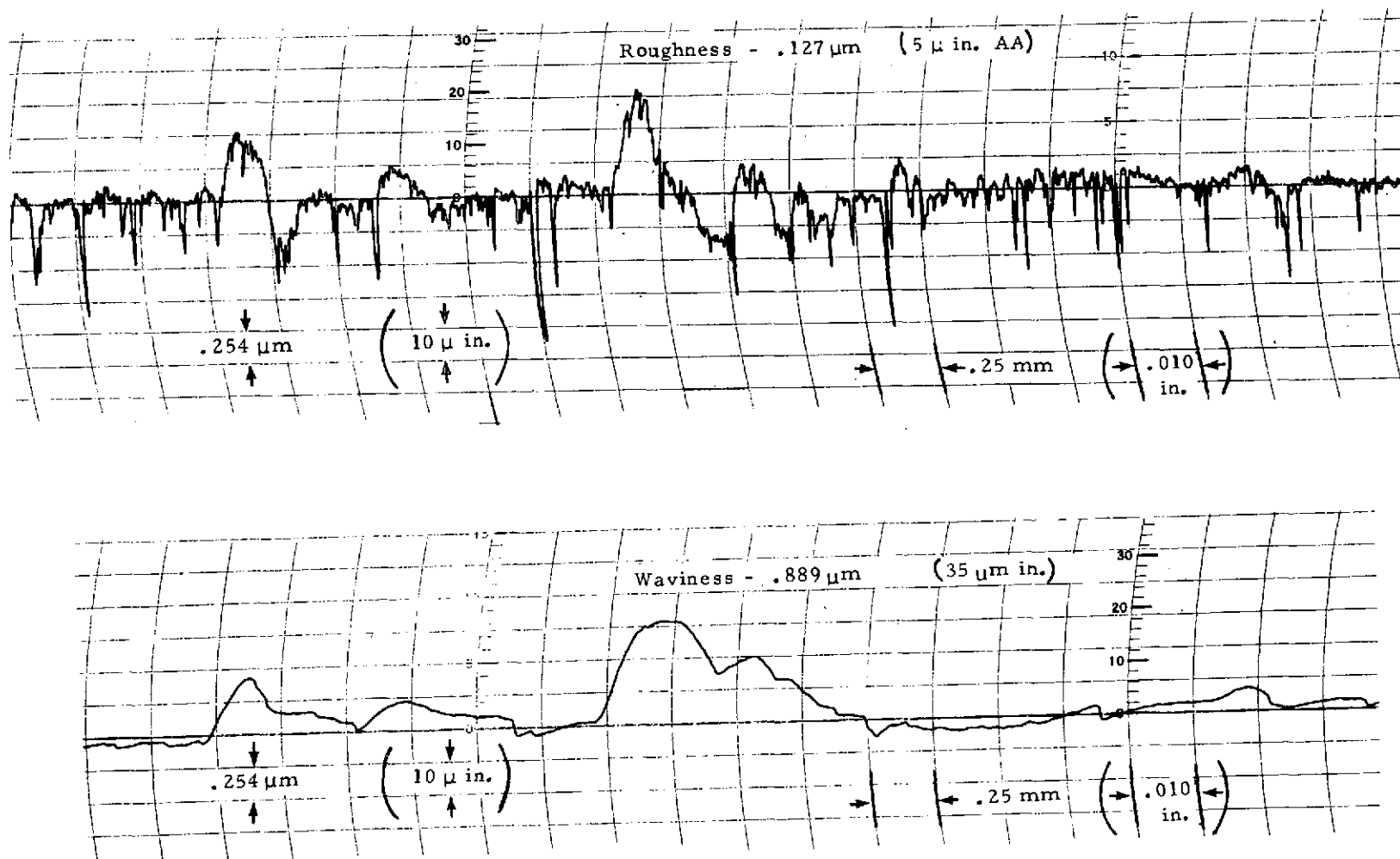


Figure 11. Forward Self-Acting Face Seal Seat Trace of Roughness and Waviness After 500-Hour Endurance Test - Trace Taken in a Radial Direction on the Seat Face Across the Running Track.

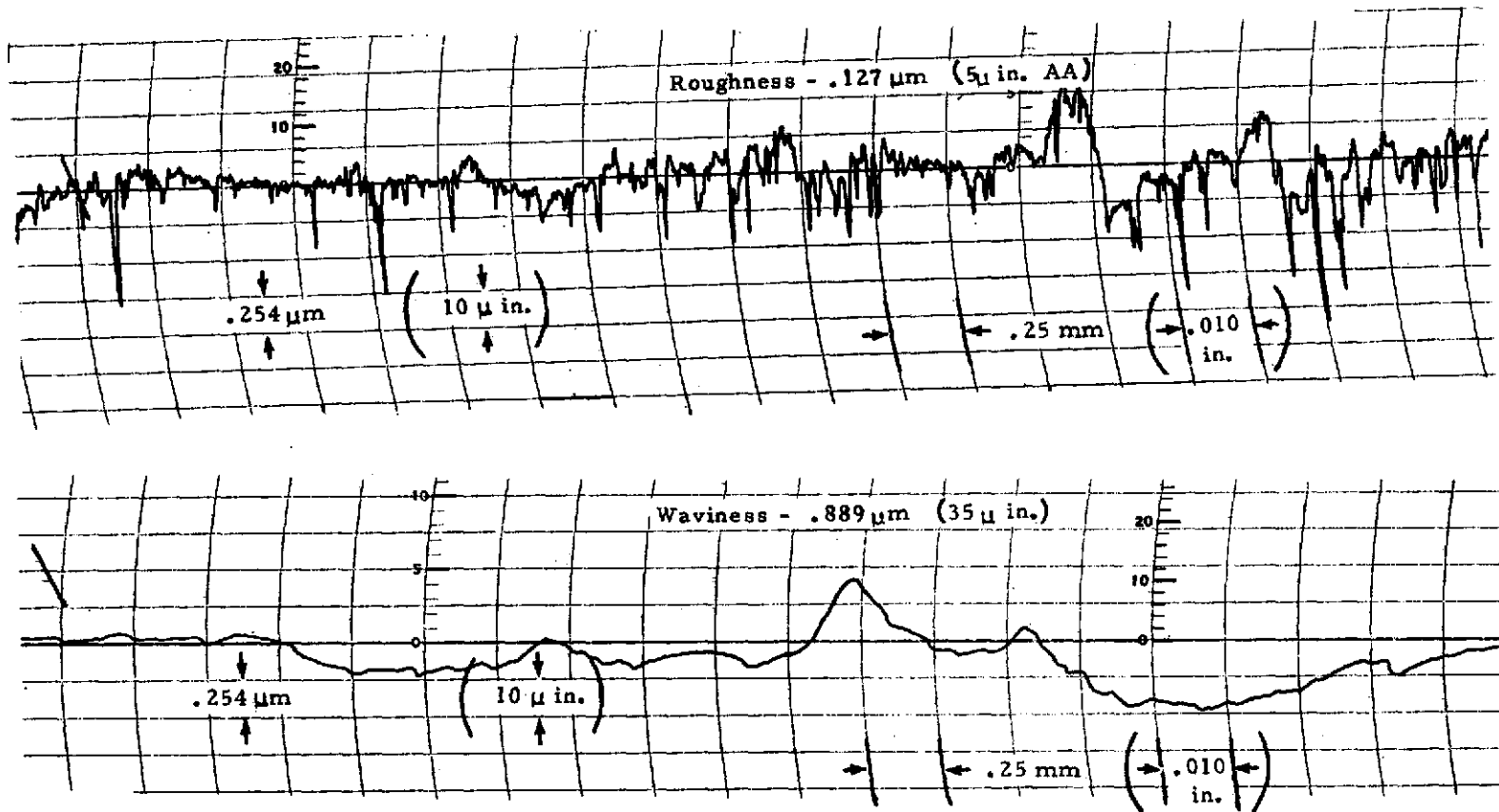


Figure 12. Aft Seal Self-Acting Face Seal Seat Trace of Roughness and Waviness After 500-Hour Endurance Test - Trace Taken in a Radial Direction on the Seat Face Across the Running Track.

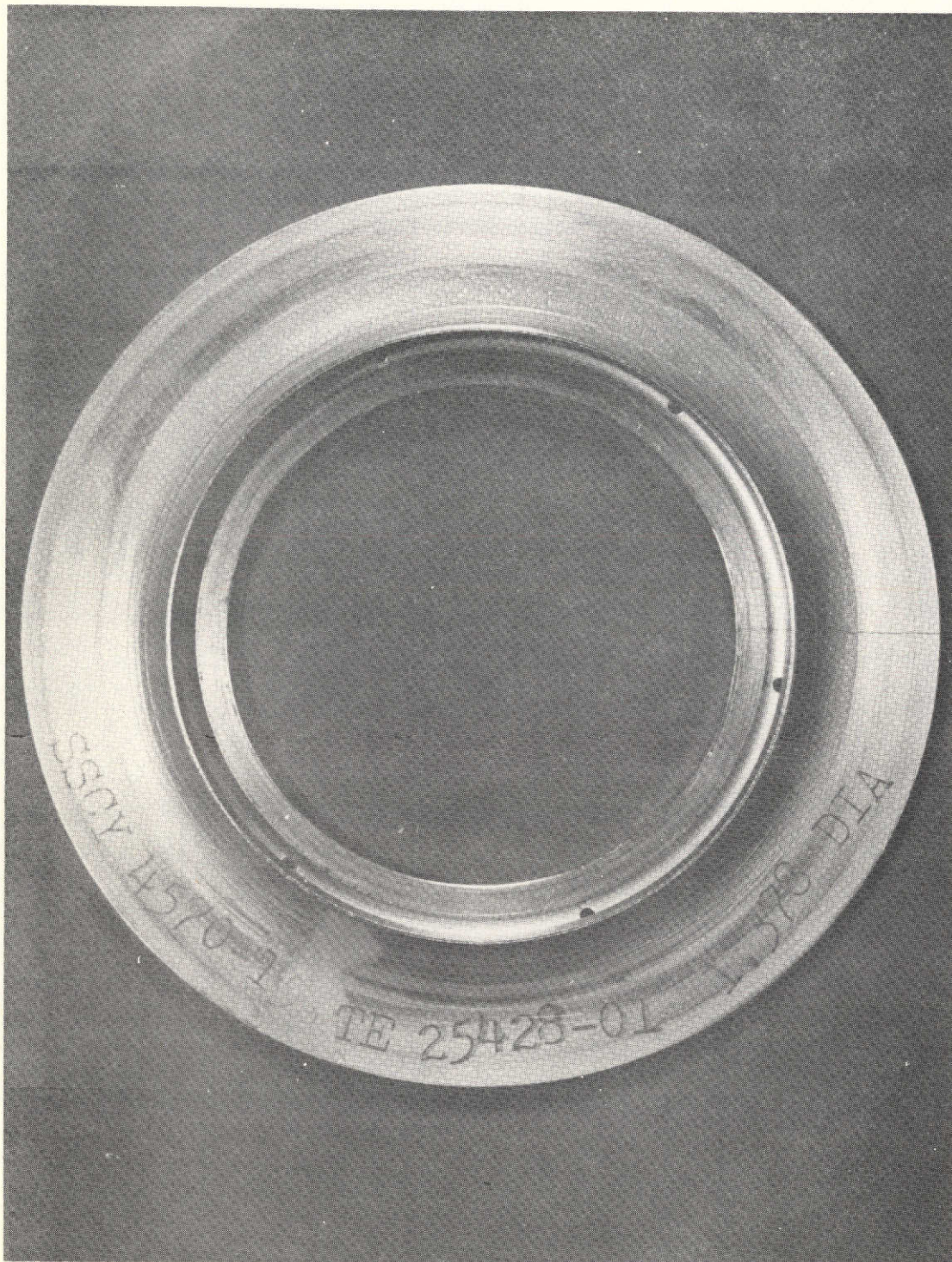


Figure 13. Cracked Oil Dam and Heat Shield, Oil Side.

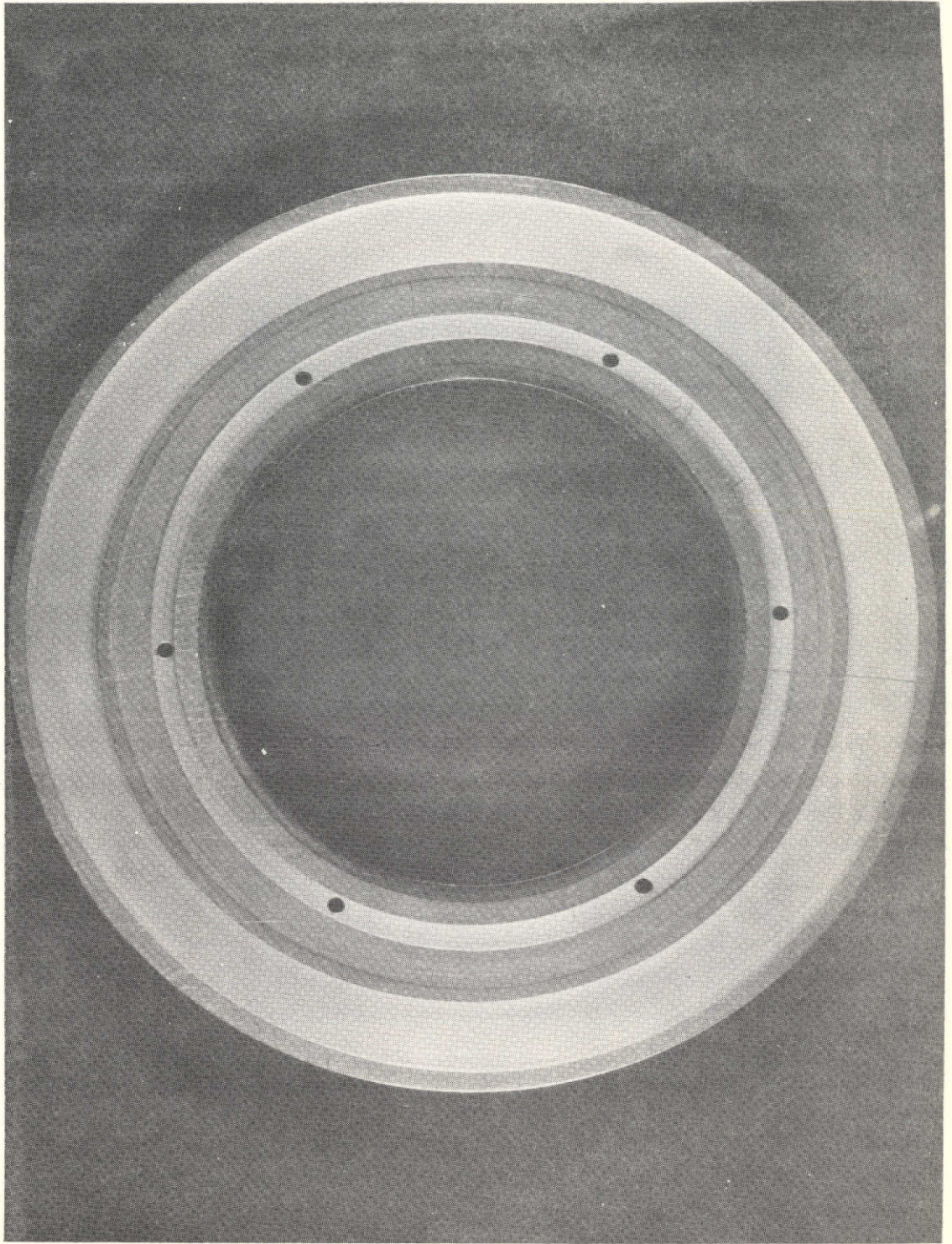


Figure 14. Cracked Oil Dam and Heat Shield, Seat Side.

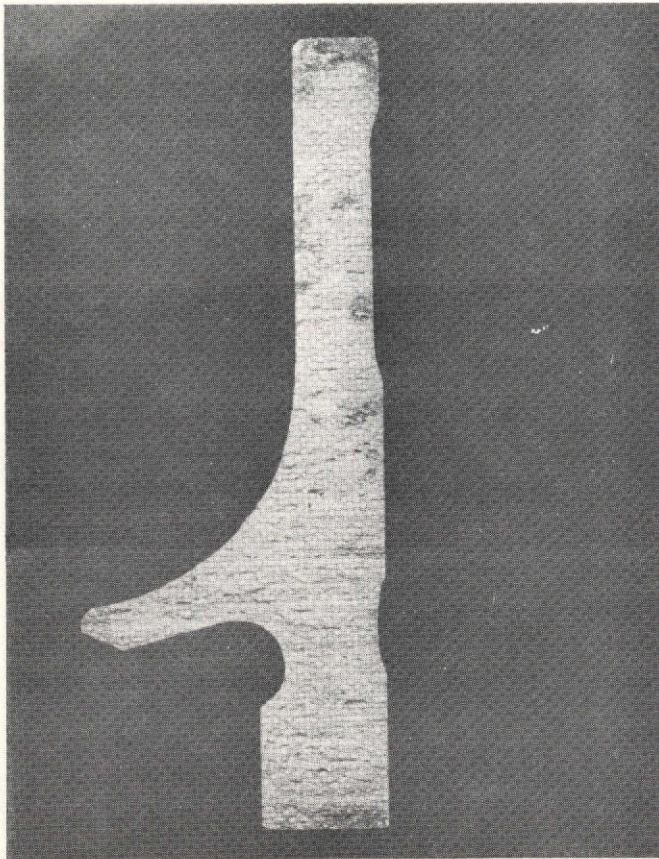


Figure 15. Oil Dam and Heat Shield, Crack Surface.

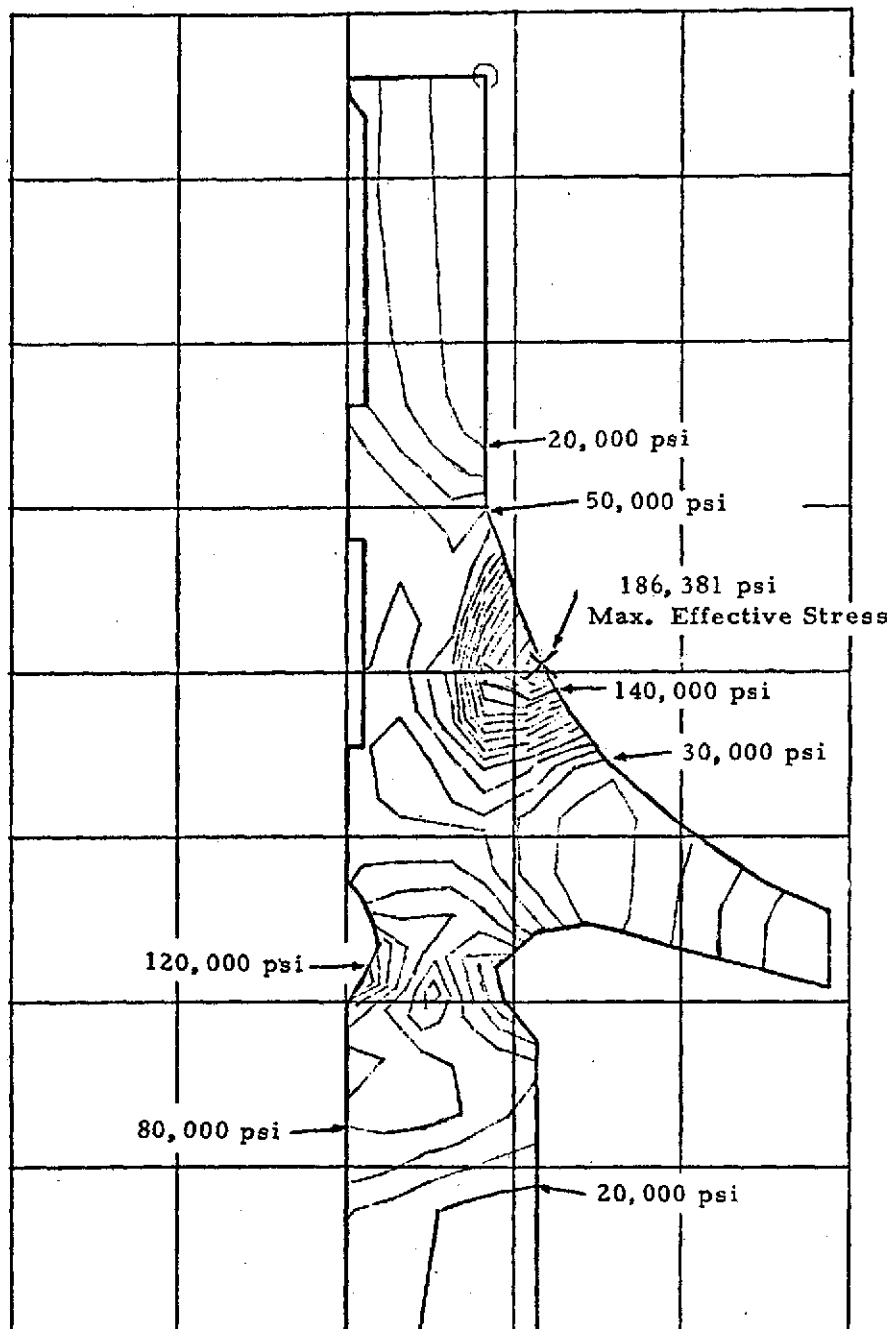


Figure 16. Stress Analysis of the Oil Dam.

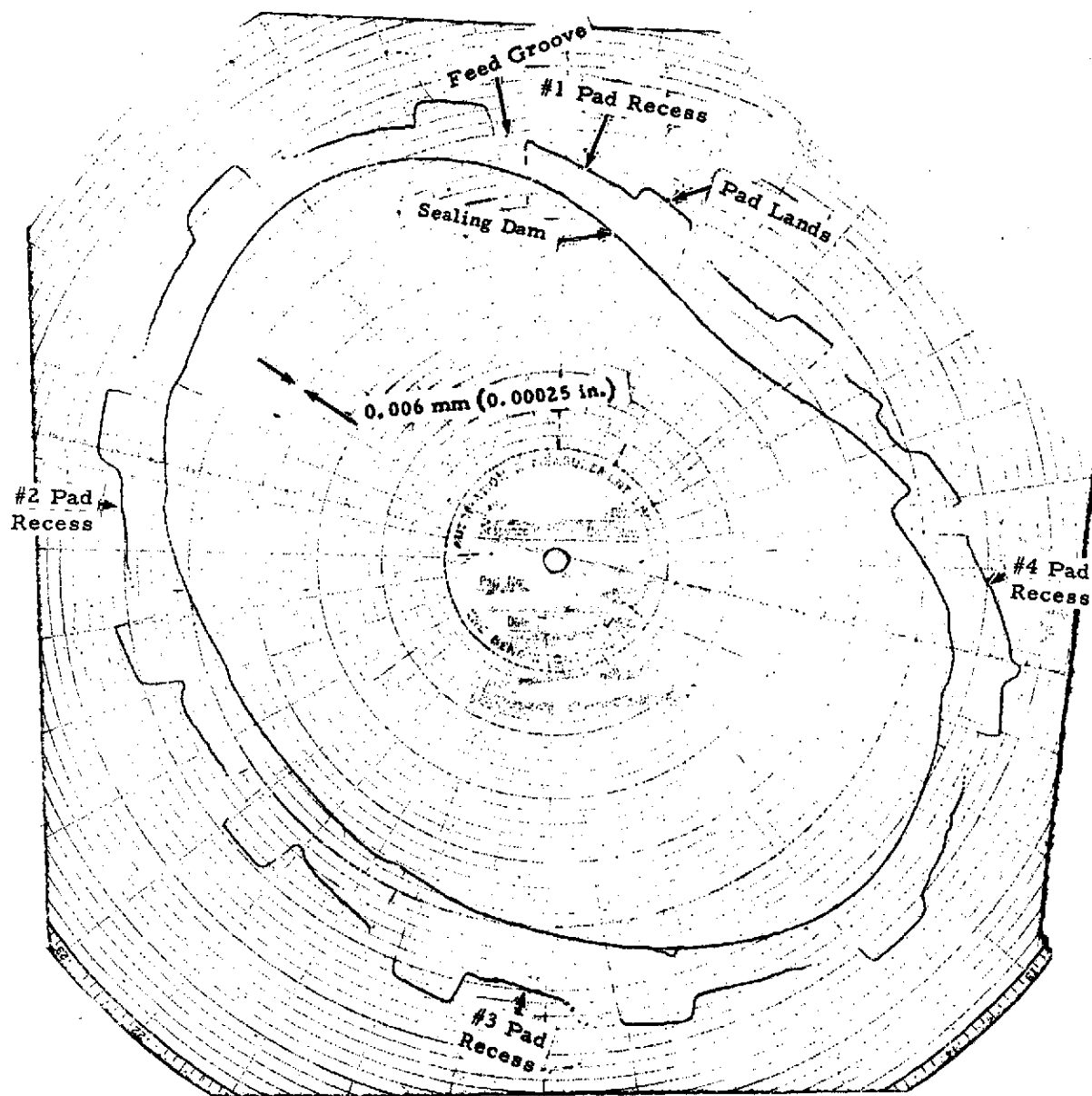


Figure 17. Trace of Forward Carbon Flatness After 500-Hour Endurance Test.

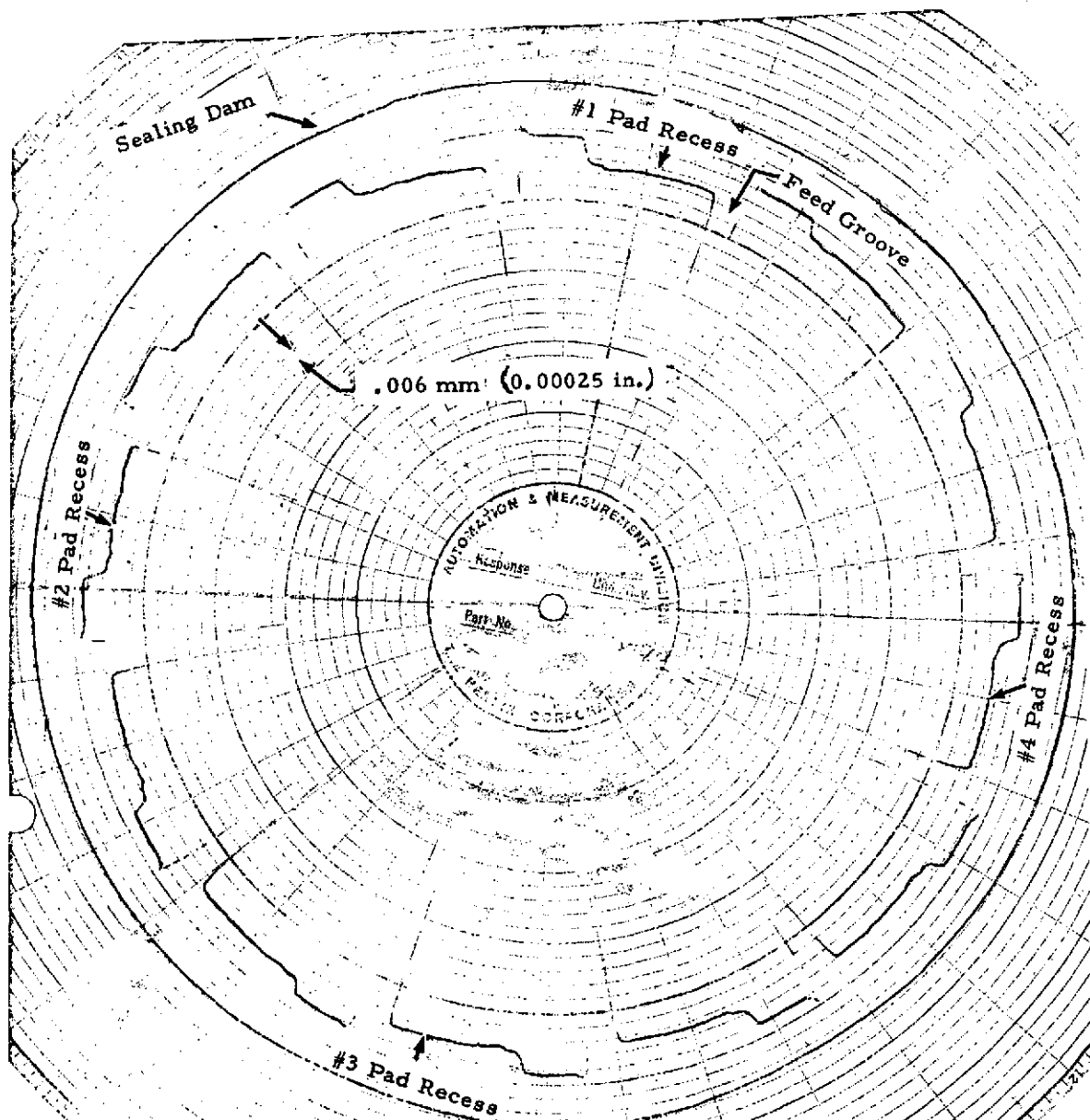


Figure 18. Trace of Aft Carbon Flatness After 500-Hour Endurance Test.

The forward carbon shifted within its retaining ring probably due to motions of the seal seat caused by the cracked oil dam and heat shield. It is theorized that this happened at the very end of the test since the components could not have operated for any length of time in this condition.

Figures 19 and 20 illustrate seal carbon and seat condition following the 500-hour endurance run. All parts were acceptable for further operation.

Temperature Test Runs

After the first 100-hour run, an attempt was made to run at elevated temperatures, and this data is reported below as separate from the 500-hour endurance test. Test conditions were as follows:

Speed - 152 m/s; (500 ft/sec, 45,500 rpm)
Air Pressure Differential - 116 N/cm² (168 psi)
Seal Temperature - 450 K (350°F)

The forward seal carbon was replaced for this test because of a chip on the back face, which was due to a loose piece of metal that had wedged in the seal between the nosepiece and windback during assembly. The chip was opposite pad 4 which had worn 0.006 mm (0.0002 in.) during the first 100 hours (Table III).

Table V presents the results of this test. Runs 1-10 were conducted at 145 m/s (475 ft/sec, 43,000 rpm) and heat was added to the air beginning with run 5. Runs 10-19 were conducted at 152 m/s (500 ft/sec). Air pressure differential was 116 N/cm² (168 psi) throughout. Each run was of 15 minute duration.

During runs 18 and 19, forward seal temperature and airflow started to fluctuate. The rig was shutdown, and inspection revealed that the forward seal carbon was worn out and the seat burned. Figure 21 illustrates the seal condition.

Airflow was excessive during the run; 0.015 kg/sec (26 scfm, .033 lb/sec). It was determined that significant air leakage was occurring at the bellows seat sealing interface. The bellows lip had worn and was not forming a perfect seal. This leakage is harmful in two ways; hot air is introduced in the bearing cavity, and the high pressure air enters under the seal and impedes the flow of the cooling oil. The seal failure, therefore, was attributed to thermal distortion of the seat caused by the air leakage past the bellows-seat interface.

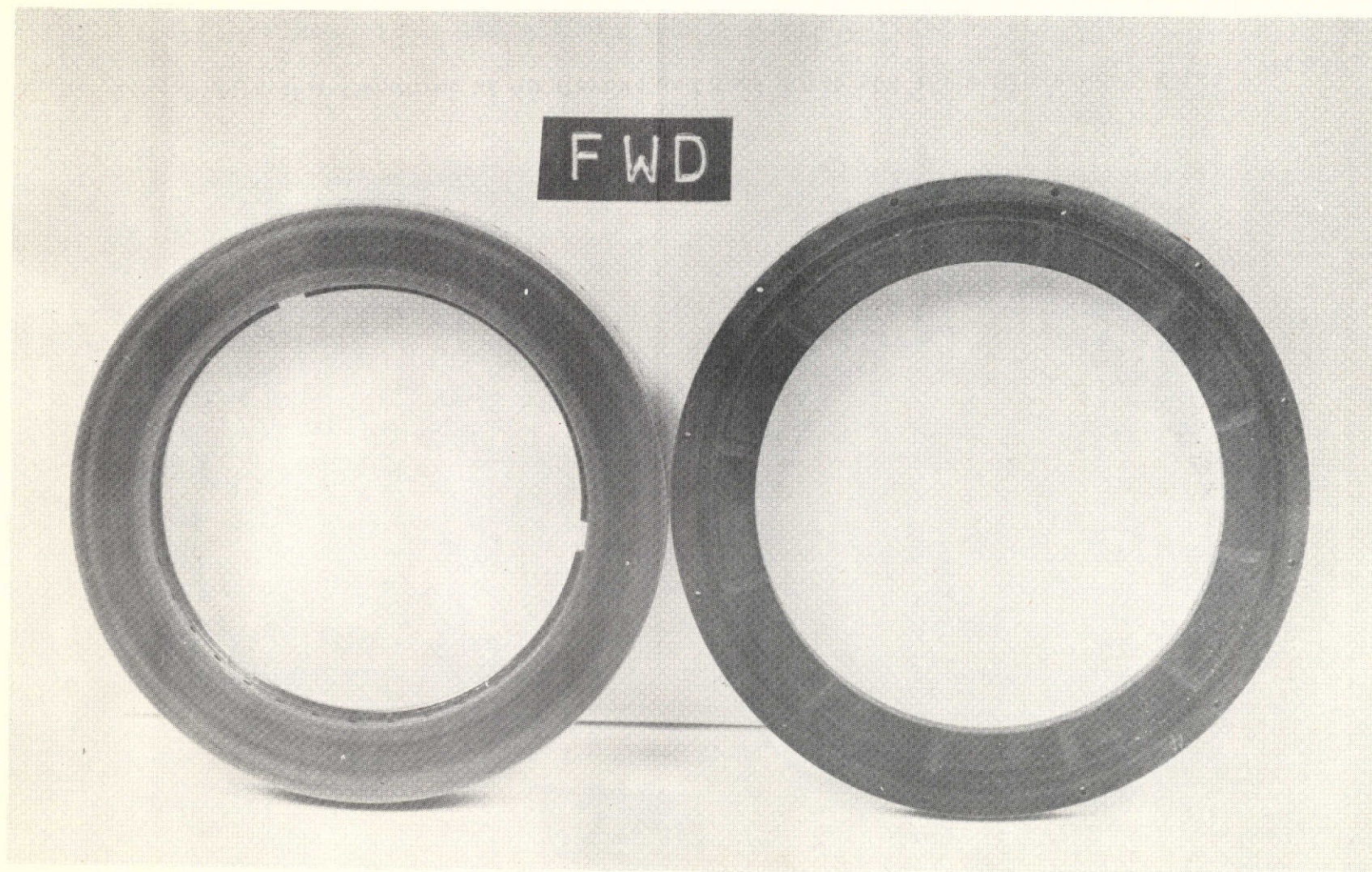


Figure 19. Condition of Forward Carbon and Seat After 500-Hour Endurance Test.

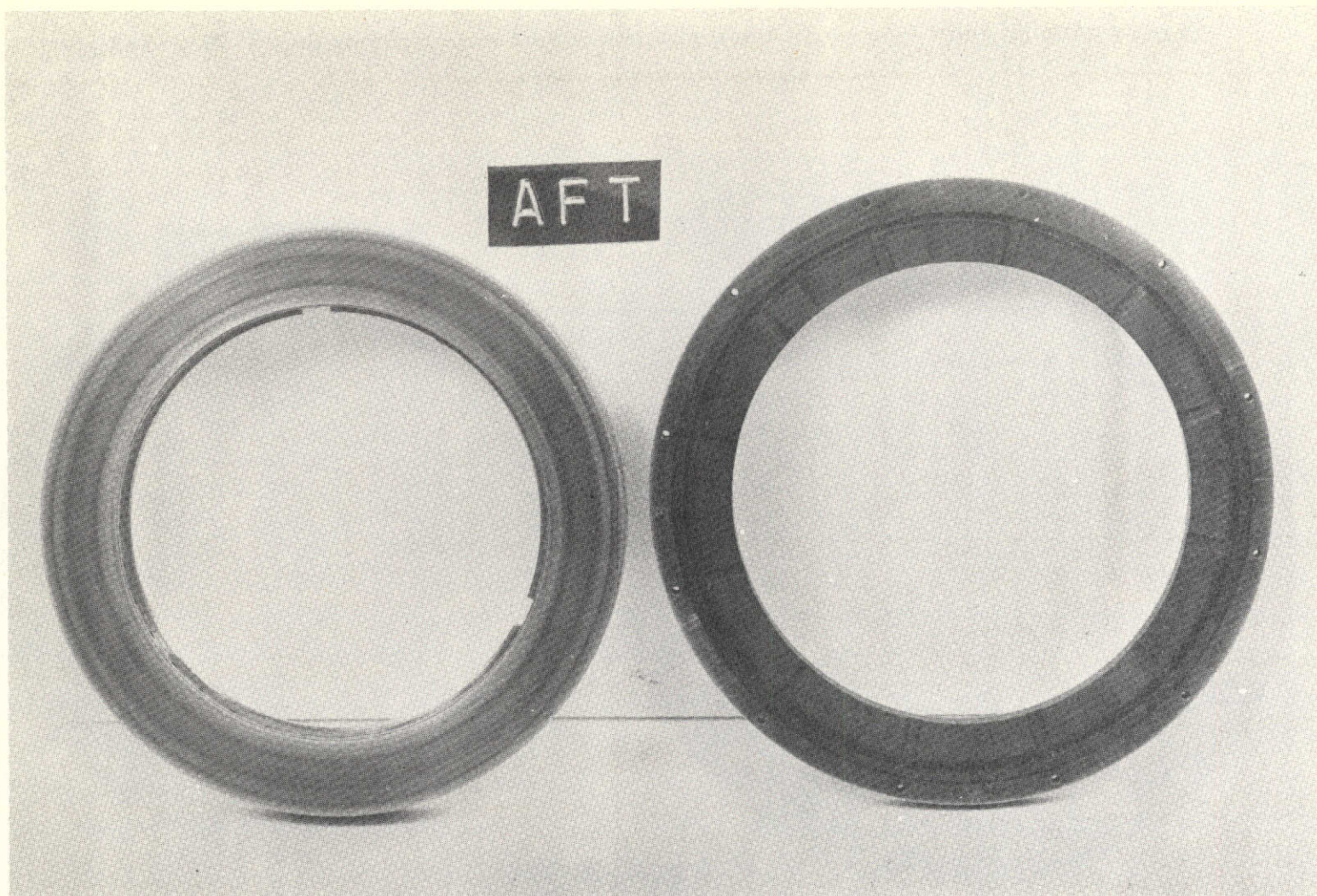


Figure 20. Condition of Aft Carbon and Seat After 500-Hour Endurance Test.

TABLE V. TEMPERATURE TEST RESULTS

Seal Sliding Speed, Max - 152 m/s (500 ft/sec, 45,500 rpm)

Pressure Differential - 116 N/cm² (168 psi)

Run	Fwd Air Temp		Fwd Seal Temp		Aft Air Temp		Aft Seal Temp		Airflow (Two Seals)		
	K	°F	K	°F	K	°F	K	°F	kg/s	scfm	lb/sec
1	339	150	382	228	312	102	358	185	.0156	27	.0344
2	336	145	382	228	316	108	365	198	.0156	27	.0344
3	339	150	388	238	318	112	364	196	.0156	27	.0344
4	340	152	390	242	319	114	381	226	.0153	26.5	.0338
5	350	170	392	246	339	150	379	222	.0153	26.5	.0338
6	372	210	404	268	374	214	392	246	.0150	26	.0331
7	400	260	421	298	410	278	402	263	.0147	25.5	.0325
8	412	280	430	314	422	300	407	272	.0144	25	.0318
9	422	300	436	325	433	320	409	276	.0147	25.5	.0325
10	422	300	439	330	437	326	412	282	.0147	25.5	.0325
11	428	310	446	344	439	330	415	289	.0153	26.5	.0338
12	428	310	446	344	439	330	415	287	.0153	26.5	.0338
13	428	310	445	343	440	332	414	286	.0150	26	.0331
14	428	310	446	344	440	332	414	286	.0150	26.5	.0338
15	428	310	446	344	440	332	414	285	.0150	26.5	.0338
16	428	310	448	346	441	334	413	284	.0150	26.5	.0338
17	428	310	448	346	441	334	414	286	.0150	26.5	.0338
18	428	310	488	418	441	334	414	286	.0162	28	.0356
19	-	-	477	400	439	330	414	284	.0168	29	.0370

ORIGINAL PAGE IS
OF POOR QUALITY

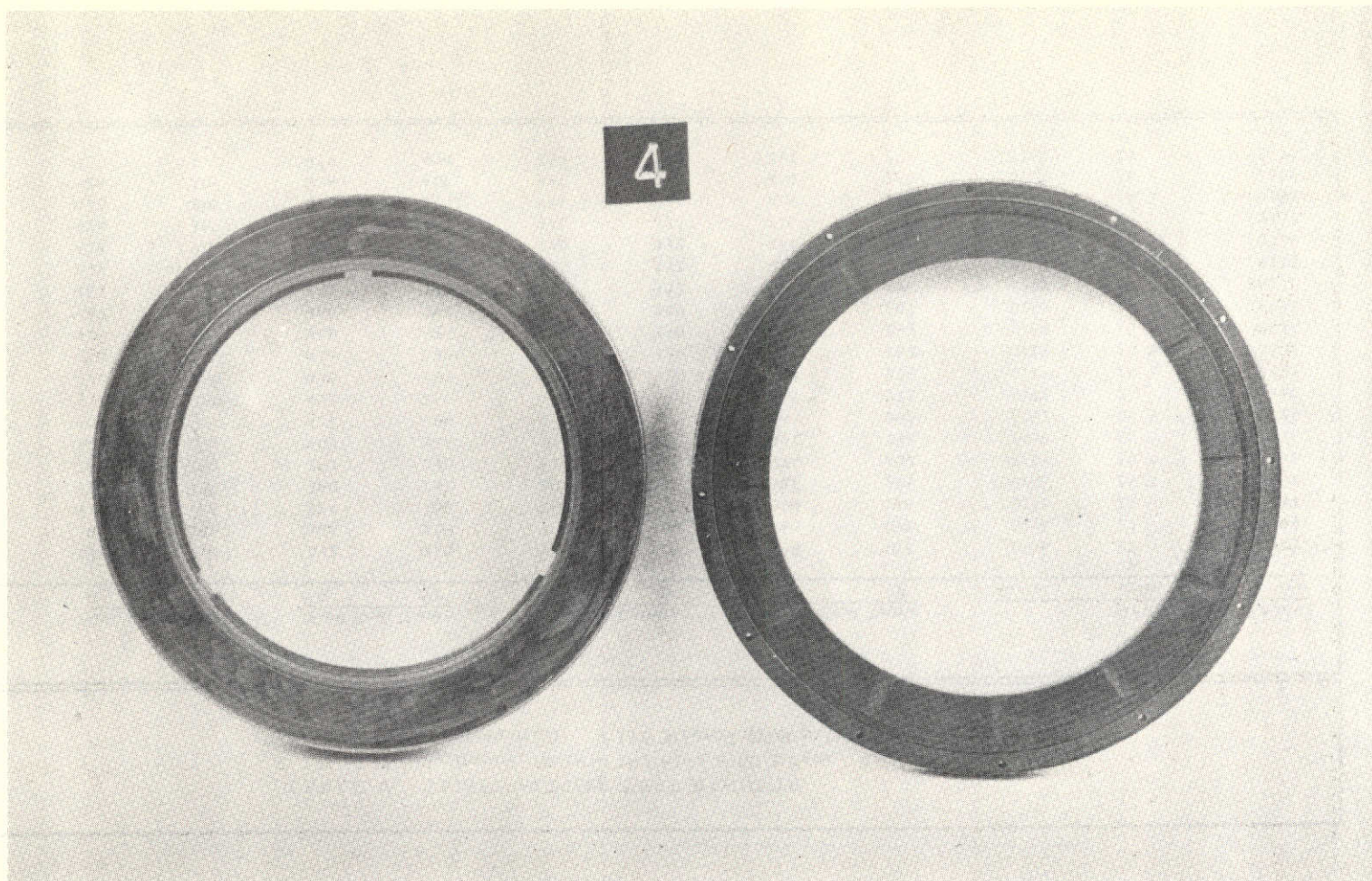


Figure 21. Condition of Forward Carbon Ring and Seat After the Temperature Test.

The face of the seat closest to the hot ambient air tends to expand faster than the face exposed to the oil side. Interruption of the cooling oil flow increases the differential expansion which rotates the outside diameter of the seat away from the carbon sealing nose, resulting in contact at the inside diameter of the sealing interface. This seat-carbon contact generates additional heat, which causes increasing distortion and increasing severe rubbing contact, with seal failure as the final result.

The aft seal was not affected by the failure. The 500-hour endurance testing then continued with the original chipped forward carbon nose-piece and a new forward seat and bellows.

Effects of Axial Runout

A series of tests were conducted to evaluate the effects of seat face axial runout. Avco Lycoming assembly practice calls for runouts less than 0.025 mm (0.001 in.) F.I.R. (Full Indicator Reading). In the runout evaluation, the test seats were manufactured with 0.051 mm (0.002 in.) runout. This was accomplished by machining one face of the seat out of parallel with the other.

Seals were operated successfully to 145 m/s (475 ft/sec, 43,000 rpm) with air pressure differential of 119 N/cm² (173 psi). Carbon and seal seat wear was negligible throughout the program indicating that the air film was maintained. Airflow was higher with the 0.051 mm (0.002 in.) runout seats as compared to the seat with runout less than 0.025 mm (0.001 in.). The higher leakage is due to slightly greater film thickness that is produced by the larger runout.

Prior to runout operation, a baseline test was conducted with seal seats correctly manufactured. Assembled seat axial runout was 0.015 mm (0.0006 in.) on the forward seat and 0.011 mm (0.00045 in.) on the aft seat. Test Results are presented in Table VI. Each run was of 15 minutes duration. Carbon and seat wear was negligible during the test.

Testing continued with the 0.051 mm (0.002 in.) axial runout seats. When measured in the free state, the runout was 0.051 mm (0.002 in.) on both the forward and aft seat. Figure 22 is an Indiron chart of seat runout in the free state. In the assembled condition, with the seats clamped to the shaft, the axial runout was reduced to 0.033 mm (0.0013 in.) on the forward seat and 0.048 mm (0.0019 in.) on the aft seat.

TABLE VI. SEAT FACE AXIAL RUNOUT EVALUATION - BASELINE TEST
 RUNOUT LESS THAN 0.025 mm (0.001 in.)

Run	Speed			Air Pressure		Cavity Pressure		Airflow(Two Seals)			Seal Temp.			
	(m/s)	(ft/sec)	(rpm)	(N/cm ² abs)	(psia)	(N/cm ² abs)	(psia)	(kg/s)	(scfm)	(lb/sec)	Fwd (K)	(°F)	Aft (K)	(°F)
1	91	300	27300	34.3	49.7	12.2	17.7	<.0006	<1.0	<.0013	356	182	255	178
2	91	300	27300	79.1	114.7	13.2	19.2	.0020	3.4	.0043	352	174	352	174
3	91	300	27300	123.9	179.7	15.7	22.7	.0040	7.0	.0089	358	185	354	176
4	91	300	27300	148.2	214.7	16.3	23.7	.0045	7.8	.0099	366	199	359	186
5	107	350	31800	34.3	49.7	12.5	18.2	<.0006	<1.0	<.0013	370	206	370	206
6	107	350	31800	79.1	114.7	13.6	19.7	.0020	3.4	.0043	367	200	368	202
7	107	350	31800	123.9	179.7	15.3	22.2	.0036	6.3	.0080	378	220	389	240
8	107	350	31800	148.2	214.7	16.3	23.7	.0043	7.5	.0096	382	228	372	210
9	122	400	36400	34.3	49.7	11.9	17.2	<.0006	<1.0	<.0013	378	220	378	220
10	122	400	36400	79.1	114.7	13.2	19.2	.0018	3.2	.0041	380	224	381	226
11	122	400	36400	123.9	179.7	15.0	21.7	.0034	5.8	.0074	388	238	387	236
12	122	400	36400	148.2	214.7	15.3	22.2	.0039	6.8	.0087	402	262	391	245
13	137	450	41000	34.3	49.7	12.9	18.7	.0006	1.0	.0013	396	253	394	250
14	137	450	41000	79.1	114.7	13.9	20.2	.0020	3.4	.0043	397	254	396	252
15	137	450	41000	123.9	179.7	15.7	22.7	.0035	6.0	.0076	412	282	402	263
16	137	450	41000	148.2	214.7	17.0	24.7	.0043	7.5	.0096	421	299	416	288
17	145	475	43000	34.3	49.7	12.9	18.7	.0006	1.0	.0013	404	266	402	263
18	145	475	43000	79.1	114.7	14.3	20.7	.0021	3.7	.0047	404	266	404	266
19	145	475	43000	123.9	179.7	15.7	22.7	.0038	6.6	.0084	422	300	407	272
20	145	475	43000	148.2	214.7	18.4	26.7	.0055	9.6	.0122	414	286	388	238

ORIGINAL PAGE IS
 OF POOR QUALITY

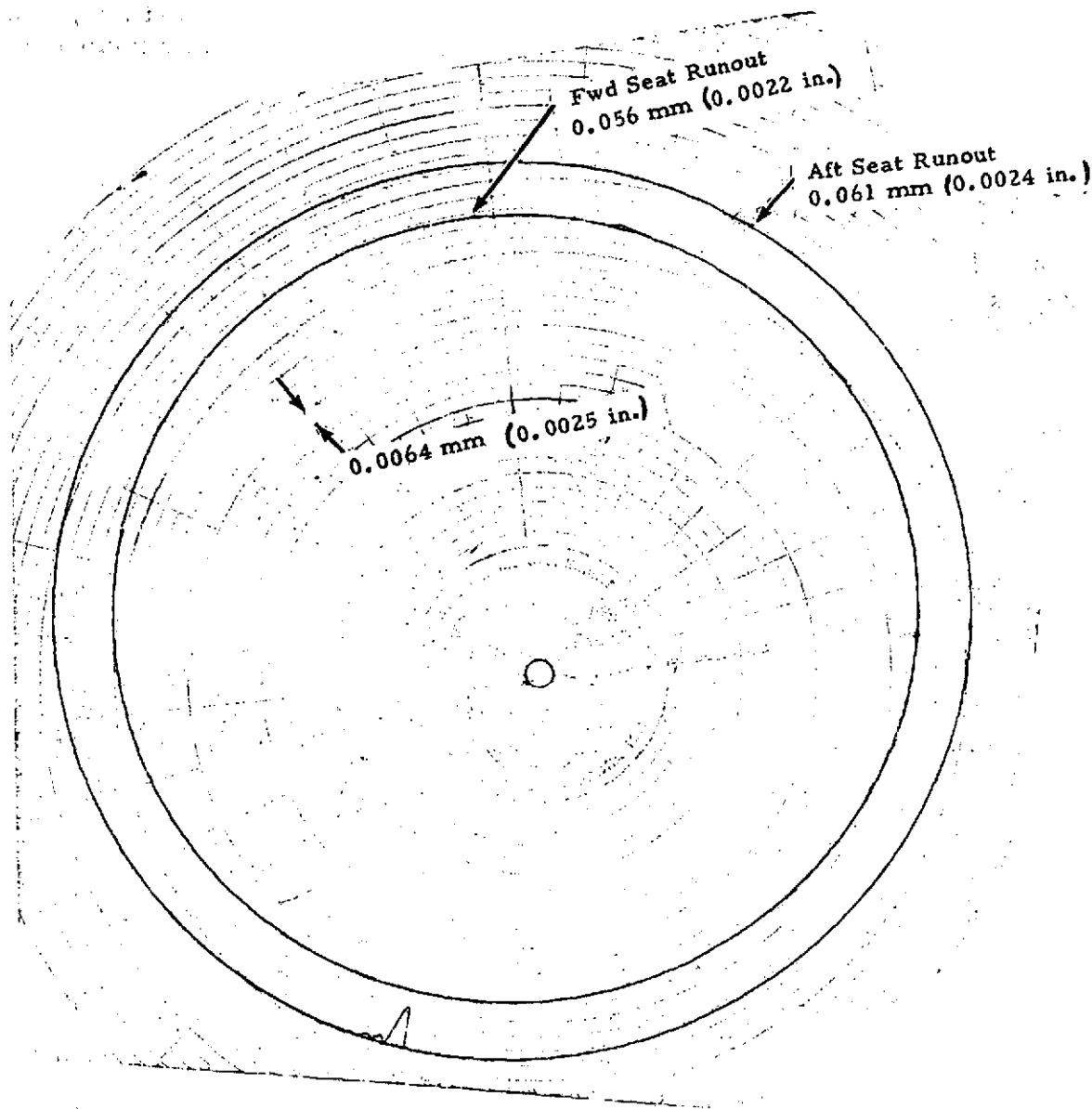


Figure 22. Seat Face Axial Runout in the Free State.

Five tests were conducted at speeds from 91 to 145 m/s (300 to 475 ft/sec) and air pressure differentials from 21 to 123 N/cm² (31 to 179 psi). Table VII presents test conditions and the resulting cavity pressures, airflows, and seal temperatures. Each test point was of 15 minute duration. Figure 23 compares baseline results to runout results at 145 m/s (475 ft/sec, 43,000 rpm) showing higher airflow with greater runout. Carbon and seal seat wear was negligible throughout the test program. Figure 24 presents static airflow checks before the baseline and runout tests.

Sand and Dust Evaluation

The purpose of this test was to demonstrate the ability of the self-acting face seal to operate successfully in a sand and dust environment. Static and rotating windbacks were incorporated in the seal design in an effort to reduce the flow rate of contaminants to the seal surfaces. Results indicated that the seals can operate stably in a severe sand and dust environment. Two windback configurations were evaluated with one clearly shown to be superior.

The contaminant used in the program was "Arizona Road Dust". Table VIII lists the specification for the dirt particle size distribution.

Prior to introducing the "Arizona Road Dust" a baseline test was conducted with no contaminants. Table IX presents test results. Each run was of 15 minute duration.

Four sand and dust tests were conducted following the baseline test. Sand was introduced at 15 minute intervals. Because sand entered in the aft air cavity, the aft seal was subjected to greater amounts of contamination than the forward. To reach the forward air cavity, sand and dust had to find its way through air passages in the bearing housing; however, significant amounts did pass through. Test parameters were as follows:

Test	Speed		Air Pressure			Amount of Sand		Time (hr)
	(m/s)	(ft/sec)	(rpm)	(N/cm ²)	(psi)	(kg/hr)	(oz/hr)	
I	122	400	36,400	109	158	0.028	1	3.5
II	122	400	36,400	105	152	0.0028	.1	6.5
III	145	475	43,000	127	184	0.0084	.3	10.0
IV	122	400	36,400	106	154	0.028	1	10.0

TABLE VII. SEAL FACE AXIAL RUNOUT EVALUATION-
RUNOUT 0.051 mm (0.002 in.)

RUN 01 0.051 mm (0.002 in.)

Test Run	Speed		Air Pressure		Cavity Pressure		Airflow (Two Seals)			Seal Temperature					
	(m/s)	(ft/sec)	(rpm)	(N/cm ² abs)	(psia)	(N/cm ² abs)	(psia)	(kg/s)	(scfm)	(lb/sec)	Fwd (°K)	(°F)	Aft (°K)	(°F)	
I	1	91	300	27,300	34.3	49.7	12.6	18.7	.0011	1.9	.0024	350	171	344	157
	2	91	300	27,300	34.3	49.7	12.6	18.7	.0012	2.0	.0025	357	183	350	170
	3	91	300	27,300	79.1	114.7	16.3	23.7	.0050	8.7	.0111	344	158	354	176
	4	91	300	27,300	79.1	114.7	17.0	24.7	.0049	8.4	.0107	352	173	360	188
	5	91	300	27,300	123.9	179.7	21.8	31.7	.0104	18.0	.0229	350	170	359	186
	6	91	300	27,300	123.9	179.7	23.2	33.7	.0107	18.5	.0236	348	167	358	184
	7	91	300	27,300	148.2	214.7	24.6	35.7	.0121	21.0	.0268	352	173	356	182
	8	91	300	27,300	148.2	214.7	24.6	35.7	.0121	21.0	.0268	353	175	359	186
II	1	107	350	31,800	34.3	49.7	12.6	18.7	.0010	1.8	.0023	367	200	361	190
	2	107	350	31,800	34.3	49.7	12.6	18.7	.0010	1.8	.0023	377	218	370	206
	3	107	350	31,800	79.1	114.7	17.0	24.7	.0046	8.0	.0102	355	179	363	194
	4	107	350	31,800	79.1	114.7	17.0	24.7	.0047	8.2	.0104	356	182	364	196
	5	107	350	31,800	123.9	179.7	22.6	32.7	.0101	17.5	.0223	364	196	367	200
	6	107	350	31,800	123.9	179.7	22.6	32.7	.0101	17.5	.0223	362	192	365	197
	7	107	350	31,800	148.2	214.7	25.3	36.7	.0121	21.0	.0268	370	206	364	196
	8	107	350	31,800	148.2	214.7	25.3	36.7	.0121	21.0	.0268	372	210	366	198
III	1	122	400	36,400	34.3	49.7	13.6	19.7	.0017	3.0	.0038	373	212	371	208
	2	122	400	36,400	34.3	49.7	13.6	19.7	.0017	3.0	.0038	372	209	368	202
	3	122	400	36,400	79.1	114.7	19.1	27.7	.0056	9.7	.0124	352	174	364	196
	4	122	400	36,400	79.1	114.7	19.1	27.7	.0058	10.0	.0127	358	184	368	202
	5	122	400	36,400	123.9	179.7	25.3	36.7	.0116	20.0	.0255	370	207	369	205
	6	122	400	36,400	123.9	179.7	25.3	36.7	.0116	20.0	.0255	376	216	371	208
	7	122	400	36,400	148.2	214.7	28.8	41.7	.0142	24.5	.0312	374	214	371	208
	8	122	400	36,400	148.2	214.7	28.8	41.7	.0145	25.0	.0318	377	219	368	202
IV	1	137	450	41,000	34.3	49.7	15.0	21.7	-	-	-	377	218	373	212
	2	137	450	41,000	34.3	49.7	15.0	21.7	-	-	-	381	226	380	224
	3	137	450	41,000	79.1	114.7	19.8	28.7	.0055	9.5	.0121	366	198	381	226
	4	137	450	41,000	79.1	114.7	20.1	29.2	.0052	9.0	.0105	367	200	377	218
	5	137	450	41,000	123.9	179.7	25.3	36.7	.0098	17.0	.0217	392	246	382	228
	6	137	450	41,000	123.9	179.7	25.3	36.7	.0098	17.0	.0217	394	248	379	222
	7	137	450	41,000	148.2	214.7	28.1	40.7	.0124	21.5	.0274	399	253	383	230
	8	137	450	41,000	148.2	214.7	28.1	40.7	.0124	21.5	.0274	398	256	380	225
V	1	145	475	43,000	34.3	49.7	15.0	21.7	.0020	3.5	.0045	389	240	384	232
	2	145	475	43,000	34.3	49.7	15.0	21.7	.0020	3.5	.0045	390	242	386	234
	3	145	475	43,000	79.1	114.7	19.4	28.2	.0061	10.5	.0134	373	212	382	228
	4	145	475	43,000	79.1	114.7	19.8	28.7	.0061	10.5	.0134	376	216	381	226
	5	145	475	43,000	123.9	179.7	25.0	36.2	.0104	18.0	.0230	402	262	368	238
	6	145	475	43,000	123.9	179.7	25.3	36.7	.0110	19.0	.0242	405	268	384	232
	7	145	475	43,000	148.2	214.7	28.8	41.7	.0136	23.5	.0299	413	283	387	237
	8	145	475	43,000	148.2	214.7	28.8	41.7	.0139	24.0	.0306	412	282	386	234

ORIGINAL PAGE IS
OF POOR QUALITY

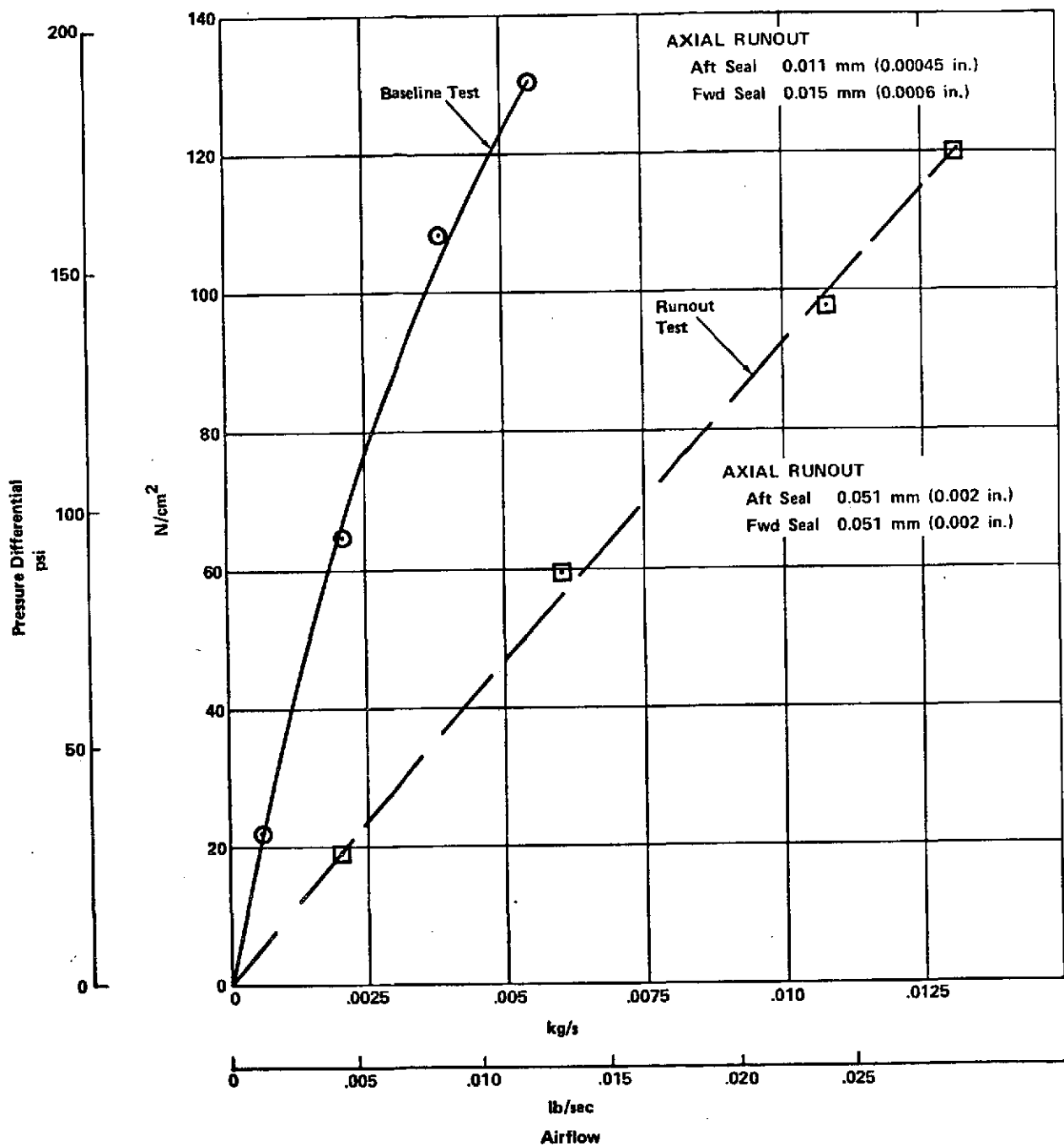


Figure 23. Airflow Through Two Seals Versus Pressure Differential
At 145 m/s (475 ft/sec) - Seat Face Axial Runout Testing.

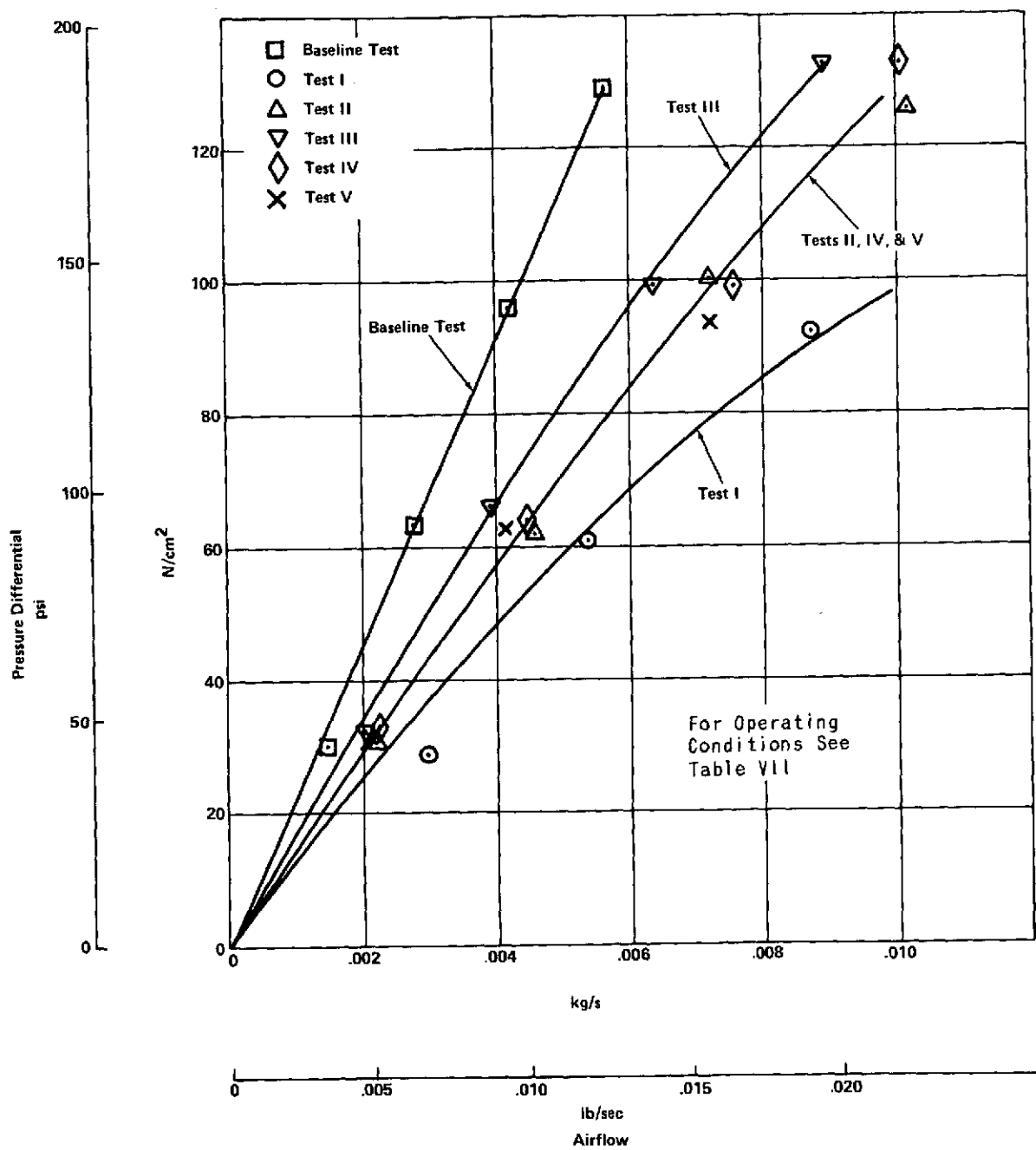


Figure 24. Static Calibrations Prior to Runout Testing.

TABLE VIII. "ARIZONA ROAD DUST" DIRT PARTICLE SIZE DISTRIBUTION

<u>Micron Size</u>	<u>Percent</u>
0-5	39 \pm 2
5-10	18 \pm 3
10-20	16 \pm 3
20-40	18 \pm 3
40-80	9 \pm 3

TABLE IX. SAND AND DUST BASELINE TEST- NO CONTAMINANTS

Run	Speed		Air Pressure		Cavity Pressure		Airflow (Two Seals			Seal Temperature			
	(m/s)	(ft/sec)	(rpm)	(N/cm ² abs)	(psia)	(N/cm ² abs)	(psia)	(kg/s)	(scfm)	(lb/sec)	Fwd (K) (°F)	Aft (K) (°F)	
1	91	300	27,300	34.3	49.7	12.1	17.5	.0006	1.0	.0013	355 178	352 174	
2	91	300	27,300	79.1	114.7	12.9	18.7	.0016	2.0	.0025	352 174	349 168	
3	91	300	27,300	123.9	179.7	13.9	20.2	.0026	4.5	.0057	359 186	350 170	
4	91	300	27,300	148.2	214.7	14.6	21.2	.0032	5.6	.0071	356 180	354 176	
5	122	400	36,400	34.3	49.7	13.2	19.2	.0006	1.0	.0013	374 214	374 214	
6	122	400	36,400	79.1	119.7	14.3	20.7	.0017	3.0	.0038	366 199	366 199	
7	122	400	36,400	123.9	179.7	15.7	22.7	.0033	5.7	.0073	373 212	368 204	
8	122	400	36,400	148.2	214.7	16.3	23.7	.0040	7.0	.0089	376 216	370 206	
9	145	475	43,000	34.3	49.7	12.9	18.7	.0006	1.0	.0013	381 226	382 228	
10	145	475	43,000	79.1	114.7	15.0	21.7	.0020	3.4	.0043	380 224	381 226	
11	145	475	43,000	123.9	179.7	16.3	23.7	.0038	6.5	.0083	392 246	380 224	
12	145	475	43,000	118.2	214.7	17.7	25.7	.0047	8.2	.0104	396 252	380 224	

ORIGINAL PAGE IS
OF POOR QUALITY

Stationary and rotating windbacks (Figures 1 and 25) are incorporated on the air side of the carbon to reduce the flow of contaminants to the sealing surfaces. Different configurations of windbacks were used for the first two tests and the last two tests. In all four tests the stationary windback pumps away from the carbon. In the first two tests the rotating windback also pumped away from the carbon. The opposite was true in the last two tests, the rotating windback pumping into the carbon. Figure 25 illustrates the windback configurations used. Testing appeared to show the second configuration with the rotating windback pumping toward the carbon is superior. It is theorized that the rotating windback creates a slightly higher pressure at the carbon than in the air cavity. The sand and dust particles are thrown out into the stationary windback by centrifugal force and pushed back to the air cavity because of the pressure differential and the thrust of the stationary windback helix.

Test I

Test I was terminated after 3.5 hours because the airflow rate had increased from 0.0029 kg/s (0.0064 lb/sec) to 0.0069 kg/s (0.0153 lb/sec). Table X presents test I data.

The aft carbon air passage grooves were impacted with sand for 25% of the circumference and spotty on the rest of the circumference. No sand was found on the lift pads of either the forward or aft seal. Sand was found around the forward and aft piston rings.

Inspection revealed carbon wear on the order of 0.0025 mm (0.0001 in.) uniformly across the lands and dam. Figure 26 shows a typical trace across a lift pad before and after testing. Figure 27 shows the seal seat scratches after testing. The scratches were extremely shallow. Figures 28 and 29 are traces of the aft seal seat taken through the contact area in a radial direction.

Test II

Test II was conducted at the same speed and pressure as test I but the amount of sand was reduced by a factor of 10 to .003 kg/hr (.1 oz/hr). The same seals from test I were used after they were cleaned.

Test parameters remained constant throughout the 6.5 hour run. Airflow remained at the same level as at the end of test I. Table XI presents test II data.

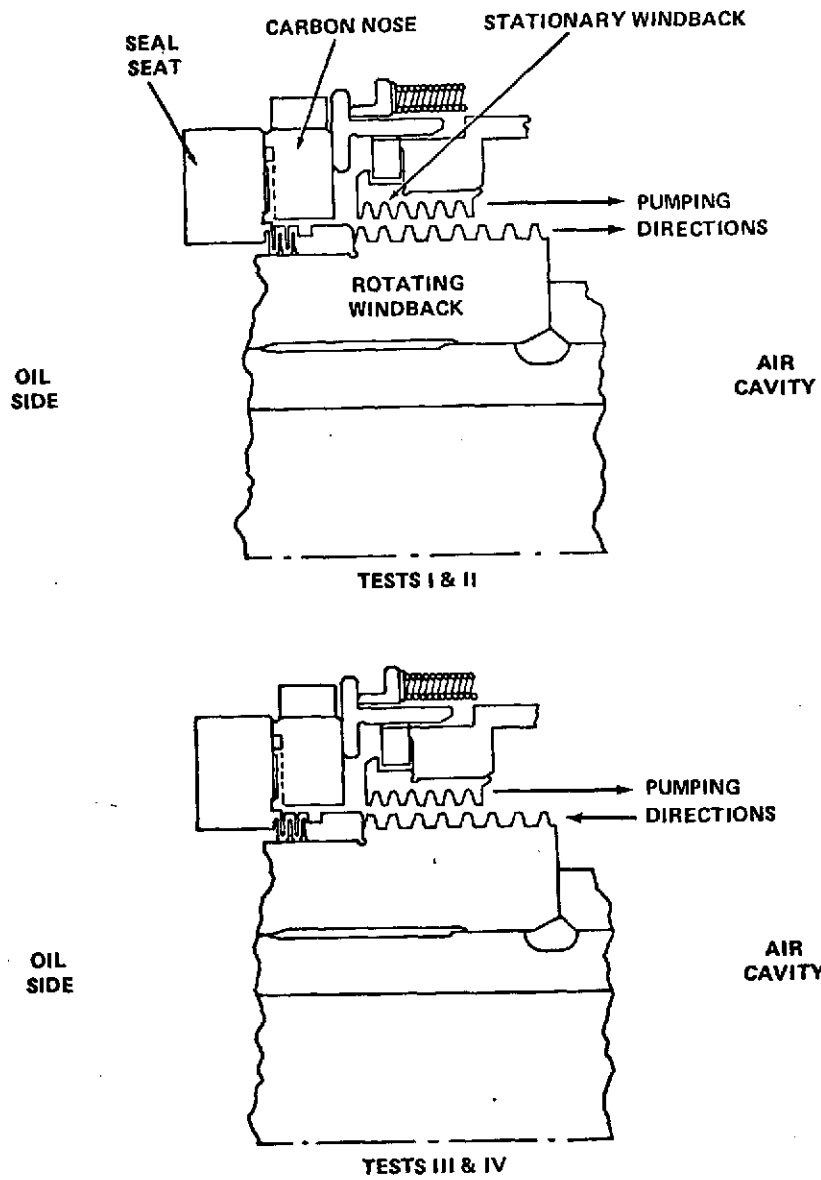


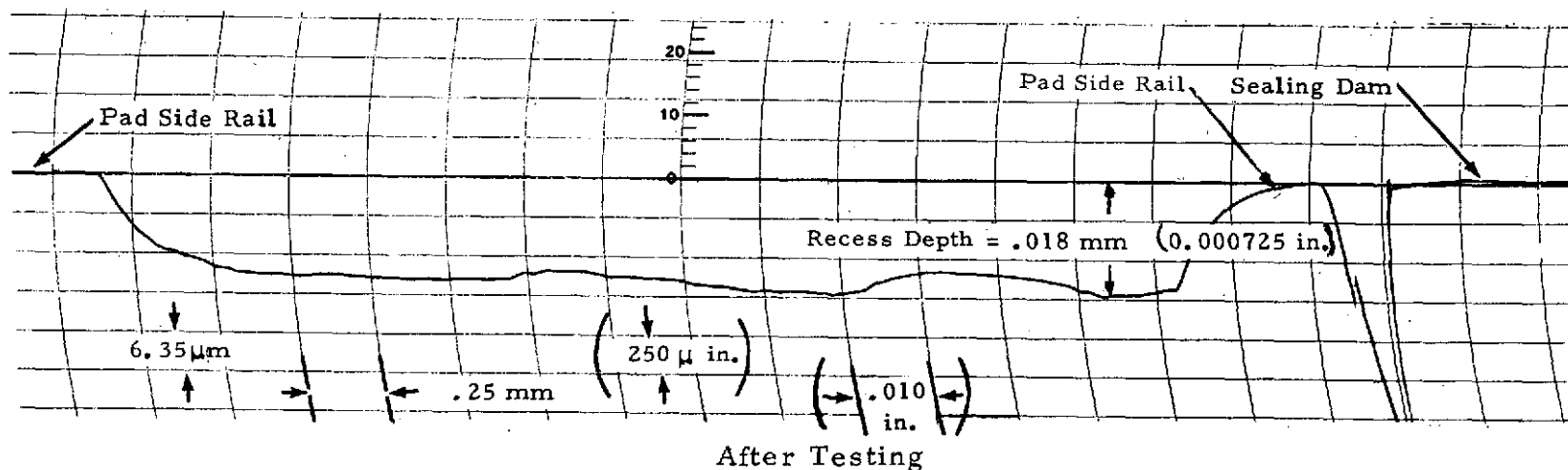
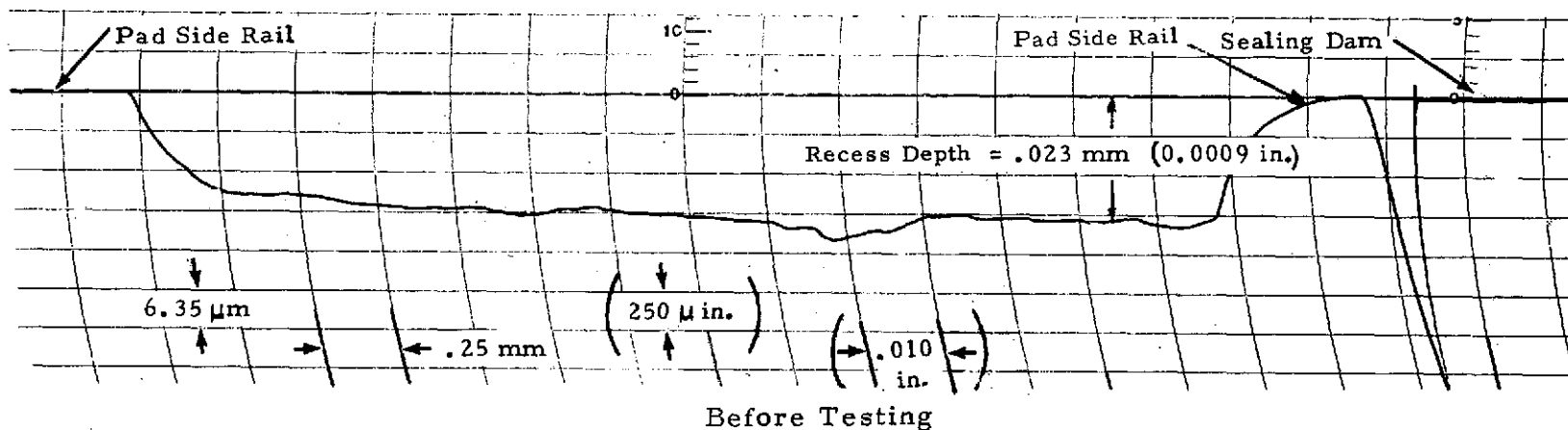
Figure 25. Sand and Dust Test Windback Configurations.

TABLE X. SAND AND DUST TEST I

Sliding Speed - 122 m/s (400 ft/sec, 36,400 rpm)
 External Air Pressure - 124 N/cm² abs (179.7 psia)
 Contaminant Flow Rate - 0.028 kg/hr (1.0 oz/hr)

Test Run	Airflow (Two Seals)			Cavity Pressure		Seal Temperature				Time (hr)
						Fwd		Aft		
	(kg/s)	(scfm)	(lb/sec)	(N/cm ² abs)	(psia)	(K)	(°F)	(K)	(°F)	
1	.003	5.6	.007	15.3	22.2	357	184	354	176	1
2	.003	5.6	.007	15.0	21.7	353	194	360	188	
3	.003	5.0	.006	15.3	22.2	368	202	367	200	
4	.003	5.1	.006	15.0	21.7	371	208	368	204	
5	.004	6.1	.008	15.6	22.7	370	207	361	190	2
6	.004	7.0	.009	15.8	22.9	371	208	361	190	
7	.005	7.8	.010	17.0	24.7	368	202	355	180	
8	.005	7.8	.010	17.0	24.7	372	210	360	189	
9	.005	9.0	.011	17.7	25.7	368	202	355	180	3
10	.005	9.5	.012	17.7	25.7	372	209	359	186	
11	.006	10.0	.013	18.1	26.2	370	206	355	179	
12	.006	11.0	.014	18.4	26.7	371	208	355	180	
13	.006	11.0	.014	18.8	27.2	372	210	356	182	
14	.007	12.0	.015	19.1	27.7	367	200	352	175	

ORIGINAL PAGE IS
OF POOR QUALITY



Sliding Speed - 122 m/s (400 ft/sec, 36,400 rpm)
 Pressure Differential - 109 N/cm² (158 psi)
 Contaminant Flow Rate - 0.028 kg/hr (1.0 oz/hr)

Figure 26. Trace of Aft Seal Lift Pad Before and After Sand and Dust Test I.

Sliding Speed - 122 m/s (400 ft/sec, 36,400 rpm)
Pressure Differential - 109 N/cm² (158 psi)
Contaminant Flow Rate - 0.028 kg/hr (1.0 oz/hr)

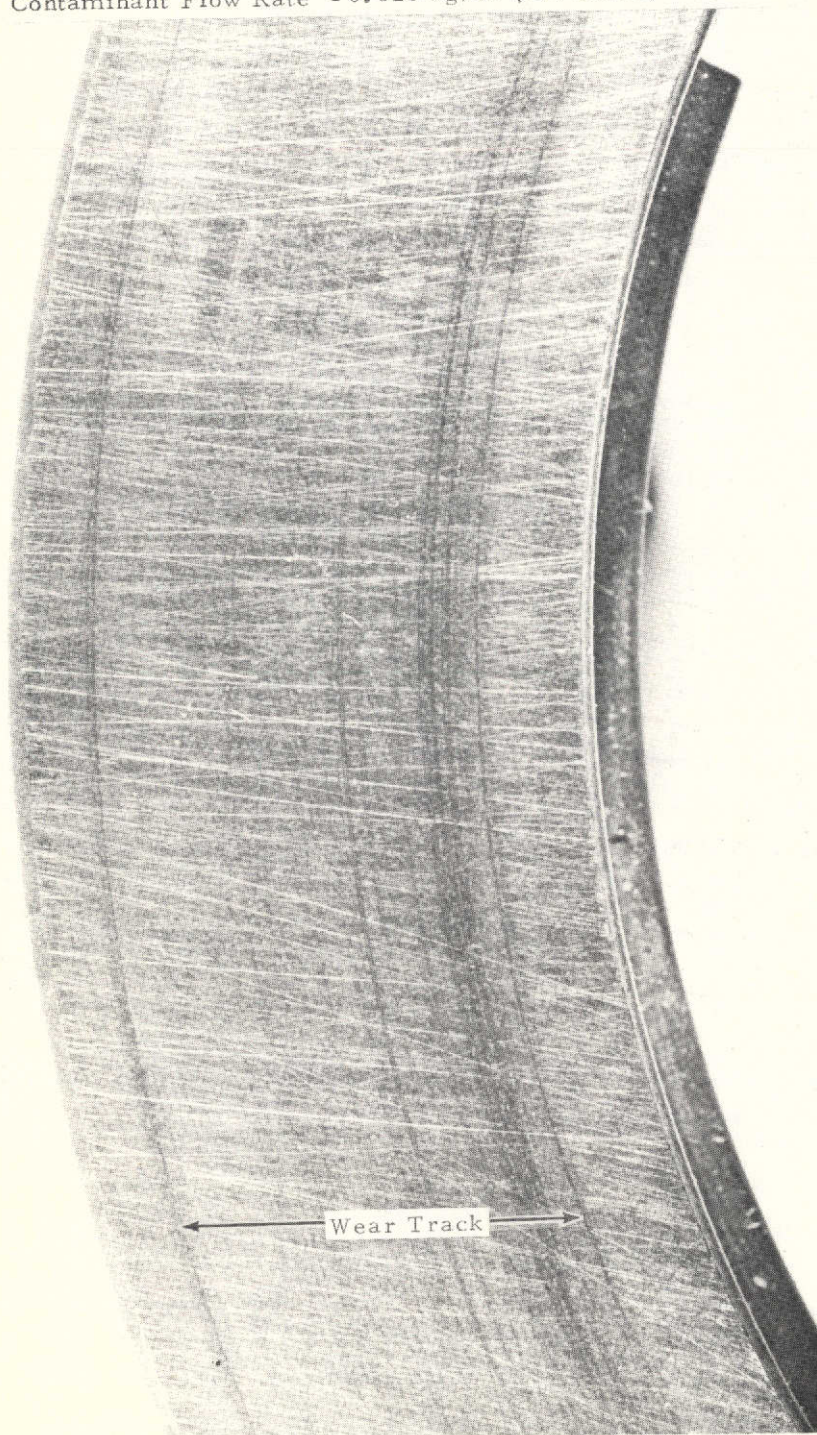
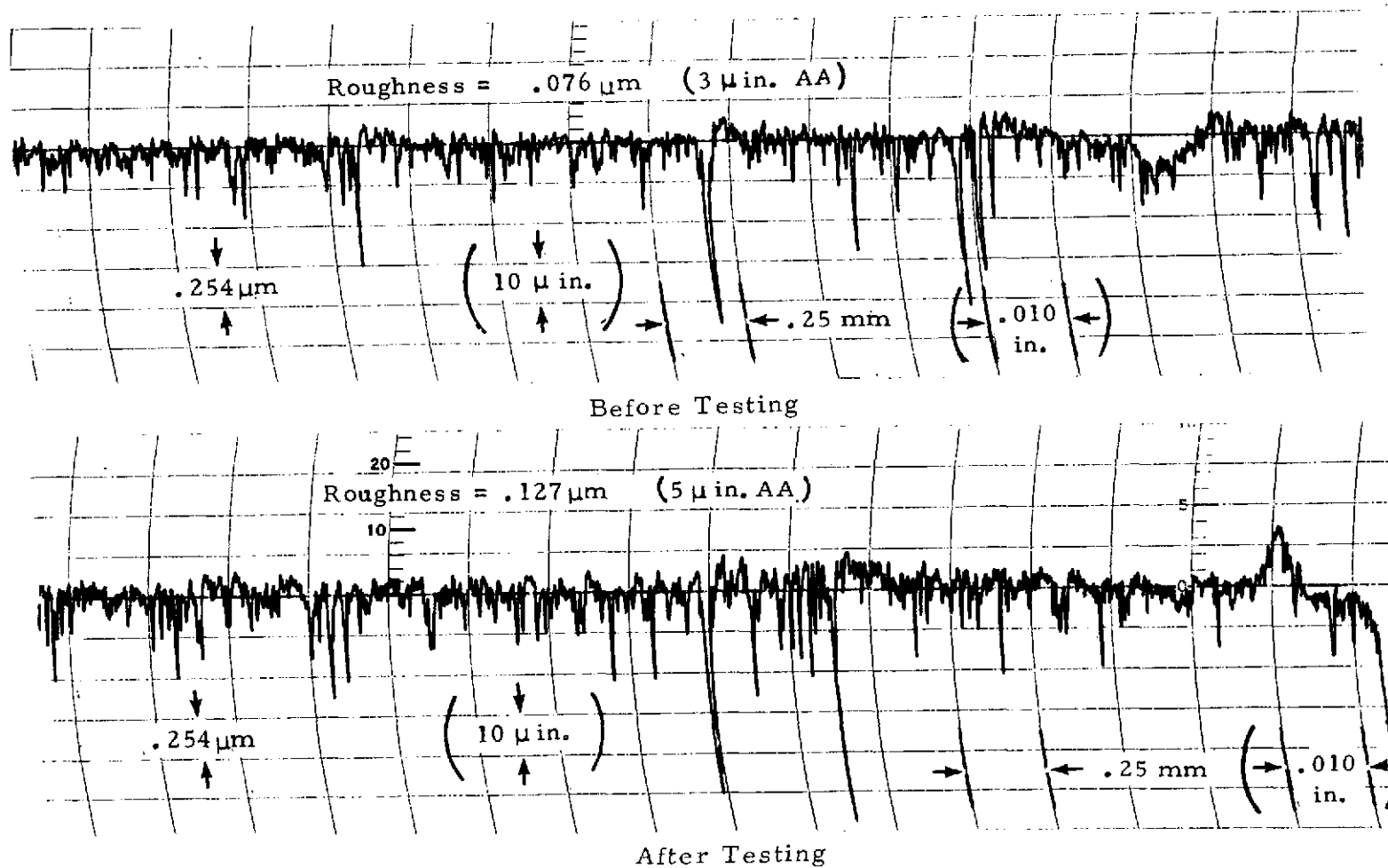


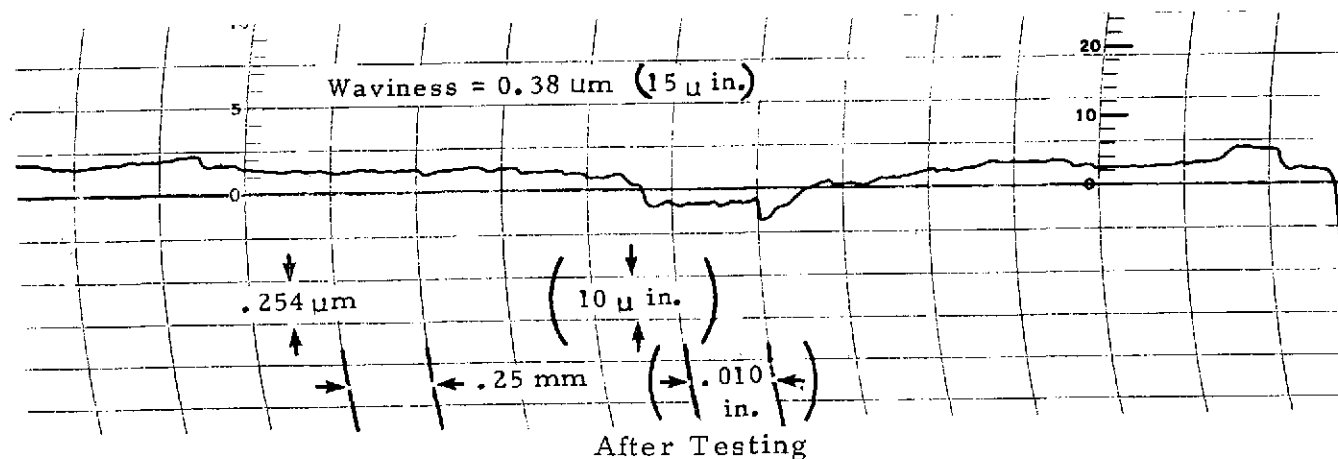
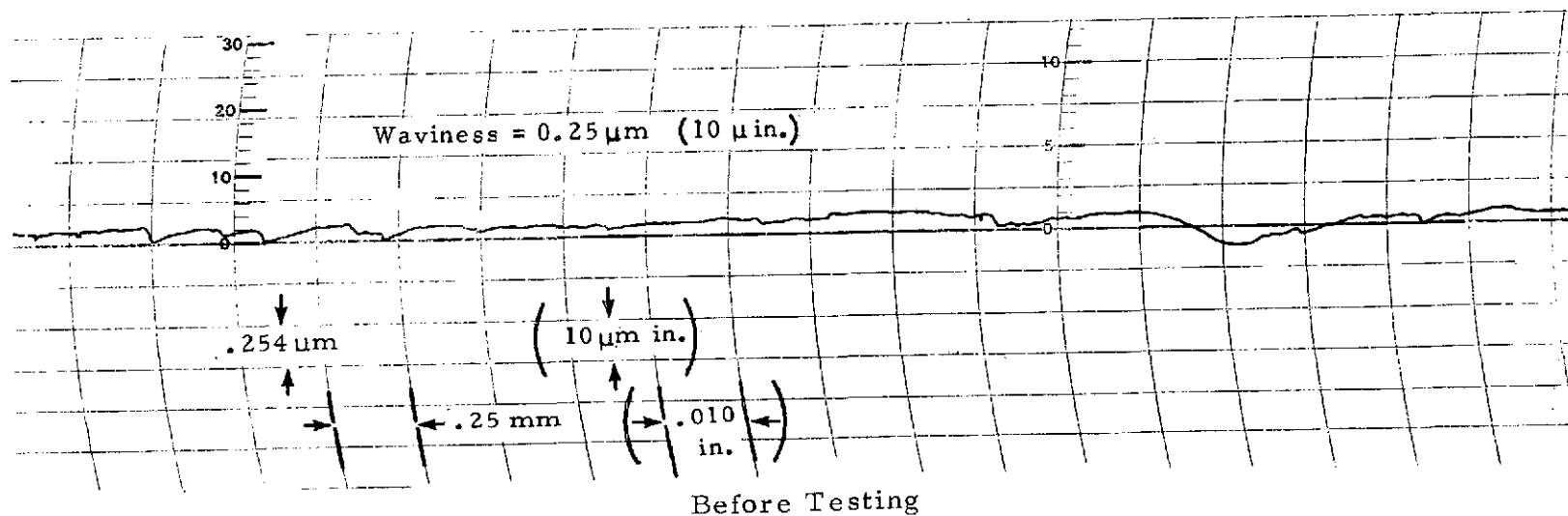
Figure 27. Aft Seal Seat After Sand and Dust Test I.

ORIGINAL PAGE IS
OF POOR QUALITY



Sliding Speed - 122 m/s (400 ft/sec, 36,400 rpm)
 Pressure Differential - 109 N/cm² (158 psi)
 Contaminant Flow Rate - 0.028 kg/hr (1.0 oz/hr)

Figure 28. Trace of Aft Seal Seat Roughness Before and After Sand and Dust Test I - Trace Taken in a Radial Direction on the Seat Face Across the Running Track.



Sliding Speed - 122 m/s (400 ft/sec , $36,400 \text{ rpm}$)
 Pressure Differential - 109 N/cm^2 (158 psi)
 Contaminant Flow Rate - 0.028 kg/hr (1.0 oz/hr)

Figure 29. Trace of Aft Seal Seat Waviness Before and After Sand and Dust Test I - Trace Taken in a Radial Direction on the Seat Face Across the Running Track.

TABLE XI. SAND AND DUST TEST II
Sliding Speed - 122 m/s (400 ft/sec, 36,400 rpm)
External Air Pressure - 124 N/cm² abs (179.7 psia)
Contaminant Flow Rate - 0.0028 kg/hr (0.1 oz/hr)

Test Run	Airflow (Two Seals)			Cavity Pressure		Seal Temperature				Time (hr)
	(kg/s)	(scfm)	(lb/sec)	(N/cm ² abs)	(psia)	Fwd		Aft		
						(K)	(°F)	(K)	(°F)	
1	.006	10.5	.013	19.1	27.7	378	220	371	208	
2	.006	11.0	.014	19.1	27.7	379	222	370	206	
3	.007	11.5	.015	19.8	28.7	376	216	366	198	
4	.007	11.5	.015	19.8	28.7	377	218	368	204	1
5	.006	11.0	.014	19.8	28.7	376	217	368	202	
6	.007	11.5	.015	19.8	28.7	374	214	366	198	
7	.007	11.5	.015	19.8	28.7	374	214	365	197	
8	.007	12.0	.015	19.8	28.7	374	214	366	198	2
9	.007	12.0	.015	19.8	28.7	374	214	367	200	
10	.007	12.0	.015	19.8	28.7	375	215	367	200	
11	.007	12.0	.015	19.8	28.7	374	214	366	198	
12	.007	11.5	.015	19.8	28.7	376	216	364	196	3
13	.007	11.5	.015	19.8	28.7	374	214	364	196	
14	.007	11.5	.015	19.8	28.7	376	216	367	200	
15	.007	11.5	.015	19.8	28.7	376	216	367	200	
16	.007	11.5	.015	19.8	28.7	377	218	368	202	4
17	.006	11.0	.014	19.8	28.7	377	218	368	202	
18	.006	11.0	.014	19.8	28.7	376	216	368	202	
19	.006	11.0	.014	19.8	28.7	376	216	367	200	
20	.006	11.0	.014	19.8	28.7	375	215	366	198	5
21	.006	11.0	.014	19.8	28.7	375	215	364	196	
22	.006	11.0	.014	19.8	28.7	376	216	365	197	
23	.006	11.0	.014	19.8	28.7	376	216	364	196	
24	.006	11.0	.014	19.8	28.7	376	216	366	198	6
25	.006	11.0	.014	19.8	28.7	377	218	367	200	
26	-	-	-	19.8	28.7	376	216	367	200	

Sand was found halfway down the rotating windback and in all threads of the stationary windback of the aft seal. No sand was found on the aft seal carbon face although there was some on the inside diameter.

On the forward seal, sand was present in the threads of both the stationary and rotating windbacks, halfway to the seal. No sand was found on the carbon face on inside diameter.

Carbon wear was negligible in test II.

Test III

For test III the rotating windbacks were replaced, and the direction of thrust was reversed (Figure 25). New carbons and seats were used. Table XII presents the test results.

On the aft seal, sand was found present on the stationary and rotating windbacks throughout their length. A light coating of sand was present in two pockets of the aft seal at approximately 12-o'clock position. Sand was also present on the bellows. The forward seal had no sand on the carbon and a light coating of sand on the windbacks. The innermost thread on the stationary windbacks was clear of sand as was the bellows.

Inspection revealed no wear on the carbons or seats.

Test IV

Test IV was conducted at the same operating conditions as test I. The only difference was the direction of thrust of the rotating windback. The test was conducted for 10 hours. Table XIII lists test results.

Seal components were in good condition following the test. Average wear on the forward seal carbon was 0.002 mm (0.00009 in.) and 0.001 mm (0.00005 in.) on the aft seal carbon.

Figures 30 and 31 show the aft seal and its housing after testing. Figure 32 shows the forward seal and its housing after testing. Figure 33 shows the seal seats and the aft rotating windback after testing.

Figures 34 through 36 show component surface texture following testing.

TABLE XII. SAND AND DUST TEST III

Sliding Speed - 145 m/s (475 ft/sec, 43,000 rpm)
 External Air Pressure - 148.2 N/cm² abs (214.7 psia)
 Contaminant Flow Rate - 0.0084 kg/hr (0.3 oz/hr)

Test Run	Airflow (Two Seals)			Cavity Pressure		Seal Temperature				Time (hr)
	(kg/s)	(scfm)	(lb/sec)	(N/cm ² abs)	(psia)	Fwd		Aft		
						(K)	(°F)	(K)	(°F)	
1	.009	15.0	.019	21.8	31.7	390	242	379	222	
2	.008	14.5	.018	21.8	31.7	396	252	383	230	
3	.008	14.0	.018	21.8	31.7	396	252	383	230	
4	.008	14.0	.018	21.8	31.7	396	252	383	230	1
5	.008	14.0	.018	21.8	31.7	394	249	380	224	
6	.008	14.0	.018	22.2	32.2	394	248	380	224	
7	.008	14.0	.018	21.8	31.7	378	220	368	202	
8	.008	14.0	.018	22.2	32.2	380	224	367	200	2
9	.009	15.0	.019	22.2	32.2	382	228	368	202	
10	.008	14.5	.018	21.8	31.7	383	230	370	206	
11	.008	14.0	.018	21.8	31.7	386	234	372	210	
12	.008	14.5	.018	21.8	31.7	386	234	372	210	3
13	.008	14.0	.018	21.8	31.7	386	234	372	210	
14	.008	14.0	.018	21.8	31.7	387	236	373	212	
15	.008	14.0	.018	21.8	31.7	387	236	373	212	
16	.008	14.0	.018	21.5	31.2	388	238	377	218	4
17	.008	14.0	.018	21.5	31.2	388	238	377	218	
18	.008	14.0	.018	21.5	31.2	389	240	378	220	
19	.008	14.0	.018	21.5	31.2	390	242	377	219	
20	.008	14.0	.018	21.8	31.7	389	240	377	218	5
21	.008	14.0	.018	21.8	31.7	389	240	378	220	
22	.008	14.0	.018	21.8	31.7	387	236	375	215	
23	.008	14.0	.018	21.8	31.7	388	238	377	218	
24	.008	14.5	.018	21.8	31.7	389	240	377	218	6
25	.008	14.5	.018	21.8	31.7	388	239	378	220	
26	.008	14.5	.018	22.2	32.2	389	240	378	220	
27	.008	14.5	.018	22.6	32.7	389	240	378	220	
28	.009	15.0	.019	22.2	32.2	388	239	377	218	7
29	.009	15.0	.019	22.6	32.7	389	240	377	218	
30	.009	15.0	.019	22.6	32.7	387	237	377	218	
31	.009	15.0	.019	22.6	32.7	389	240	377	218	
32	.009	15.0	.019	22.6	32.7	389	240	377	218	8
33	.009	15.0	.019	22.6	32.7	389	240	377	218	
34	.009	15.0	.019	22.6	32.7	389	240	377	218	
35	.009	15.0	.019	22.2	32.2	391	244	379	222	
36	.009	15.0	.019	22.6	32.7	390	242	378	220	9
37	.009	15.0	.019	22.6	32.7	390	243	378	220	
38	.009	15.0	.019	22.6	32.7	389	240	377	218	
39	.009	15.0	.019	22.6	32.7	388	238	376	216	
40	.009	15.0	.019	22.6	32.7	389	240	377	218	10

TABLE XIII. SAND AND DUST TEST IV

Sliding Speed - 122 m/s (400 ft/sec, 36,400 rpm)
 External Air Pressure - 124 N/cm² abs (179.7 psia)
 Contaminant Flow Rate - 0.028 kg/hr (1.0 oz/hr)

Test Run	Airflow (Two Seals)			Cavity Pressure		Fwd Seal Temp.		Time (hr)
	(kg/s)	(scfm)	(lb/sec)	(N/cm ² abs)	(psia)	(K)	(°F)	
1	.006	10.3	.013	18.4	26.7	371	208	
2	.006	10.4	.013	18.7	27.2	370	206	
3	.006	10.4	.013	18.7	27.2	272	209	
4	.006	10.3	.013	18.7	27.2	373	212	1
5	.006	10.1	.013	18.6	26.9	374	214	
6	.006	9.9	.013	18.5	26.8	374	214	
7	.005	9.4	.012	18.4	26.7	376	216	
8	.005	9.0	.011	18.4	26.7	378	220	2
9	.005	9.0	.011	18.2	26.5	379	222	
10	.005	9.2	.012	18.4	26.7	378	220	
11	.005	8.9	.011	18.4	26.7	378	220	
12	.005	8.5	.011	18.4	26.7	379	222	3
13	.005	8.4	.011	18.4	26.7	379	222	
14	.005	8.4	.011	18.1	26.2	379	222	
15	.005	8.2	.010	17.7	25.7	379	222	
16	.005	8.3	.011	17.7	25.7	379	222	4
17	.005	8.2	.010	17.7	25.7	382	228	
18	.005	8.3	.011	17.7	25.7	381	226	
19	.005	8.4	.011	17.7	25.7	380	224	
20	.005	8.0	.010	17.7	25.7	382	227	5
21	.005	8.0	.010	17.7	25.7	381	226	
22	.005	8.0	.010	17.7	25.7	381	226	
23	.005	8.2	.010	17.7	25.7	391	226	
24	.005	8.2	.010	17.7	25.7	380	224	6
25	.005	8.2	.010	17.7	25.7	380	224	
26	.005	8.2	.010	17.7	25.7	381	226	
27	.005	8.2	.010	17.7	25.7	381	226	
Shut Down								
28	.005	8.5	.011	17.7	25.7	376	216	7
29	.005	8.5	.011	17.7	25.7	378	220	
30	.005	8.2	.010	17.7	25.7	378	220	
31	.005	8.2	.010	17.7	25.7	378	220	
32	.005	8.2	.010	17.7	25.7	378	220	8
33	.005	8.2	.010	17.7	25.7	378	220	
34	.005	8.2	.010	17.4	25.2	378	220	
35	.005	8.2	.010	17.4	25.2	379	222	
36	.005	8.2	.010	17.4	25.2	379	222	9
37	.005	8.5	.011	17.4	25.2	378	220	
38	.005	8.5	.011	17.4	25.2	380	224	
39	.005	8.5	.011	17.4	25.2	379	222	
40	.005	8.5	.011	17.4	25.2	378	220	10

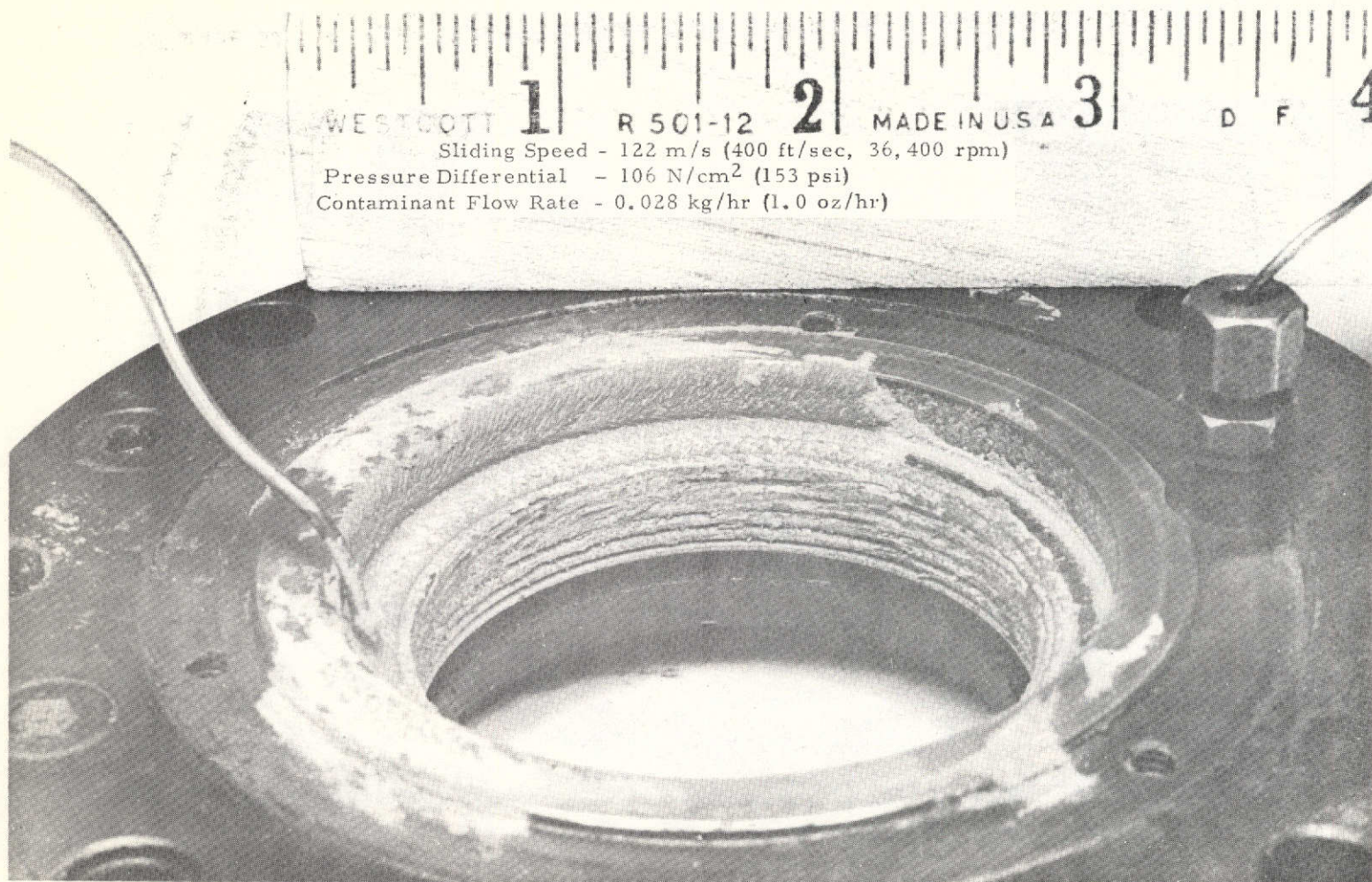


Figure 30. Aft Seal After Sand and Dust Test IV Viewed From the Air Side.

Sliding Speed - 122 m/s (400 ft/sec, 36,400 rpm)
Pressure Differential - 106 N/cm² (153 psi)
Contaminant Flow Rate - 0.028 kg/hr (1.0 oz/hr)

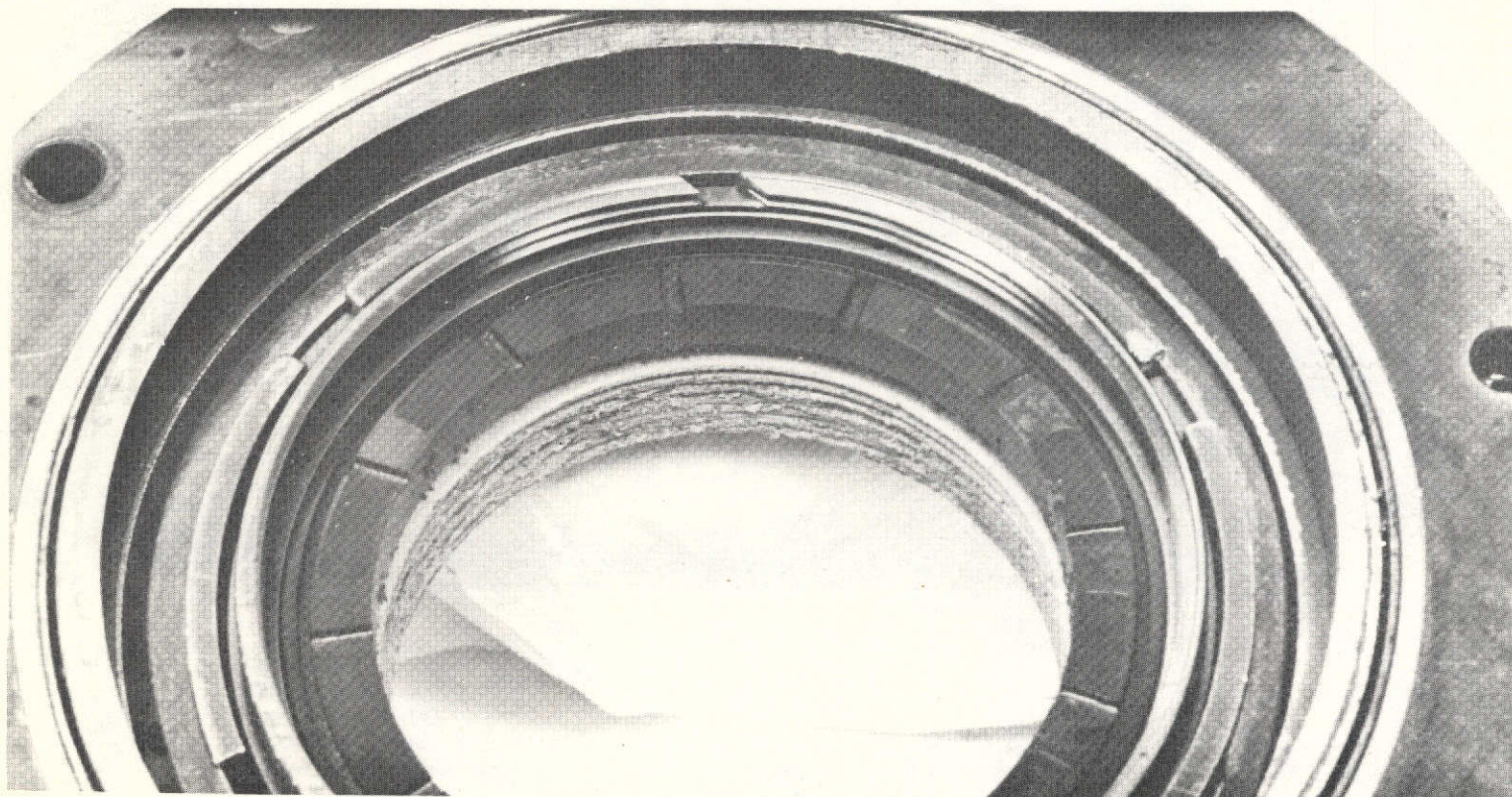


Figure 31. Aft Seal After Sand and Dust Test IV Viewed From the Oil Side.

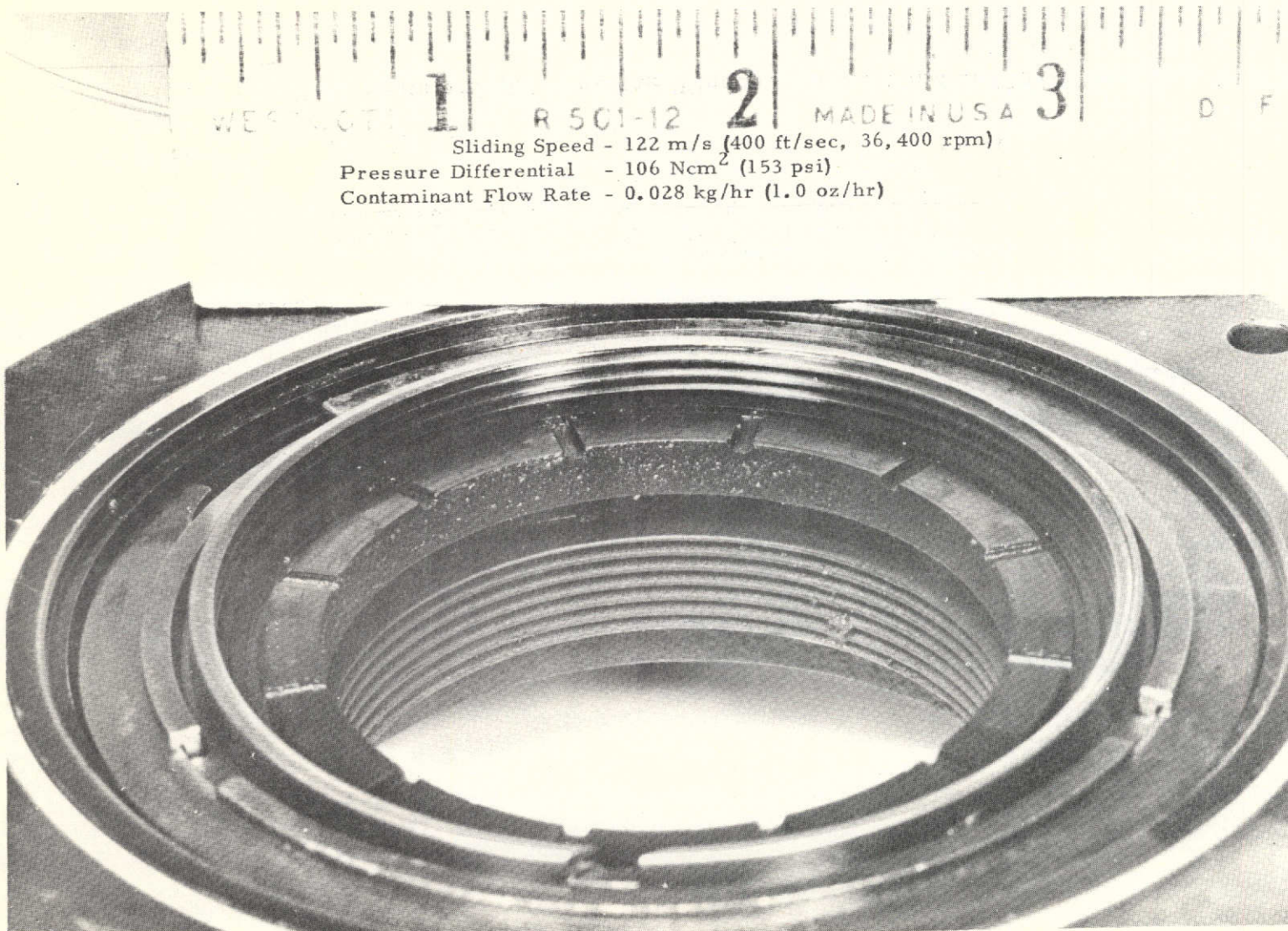


Figure 32. Forward Seal After Sand and Dust Test IV.

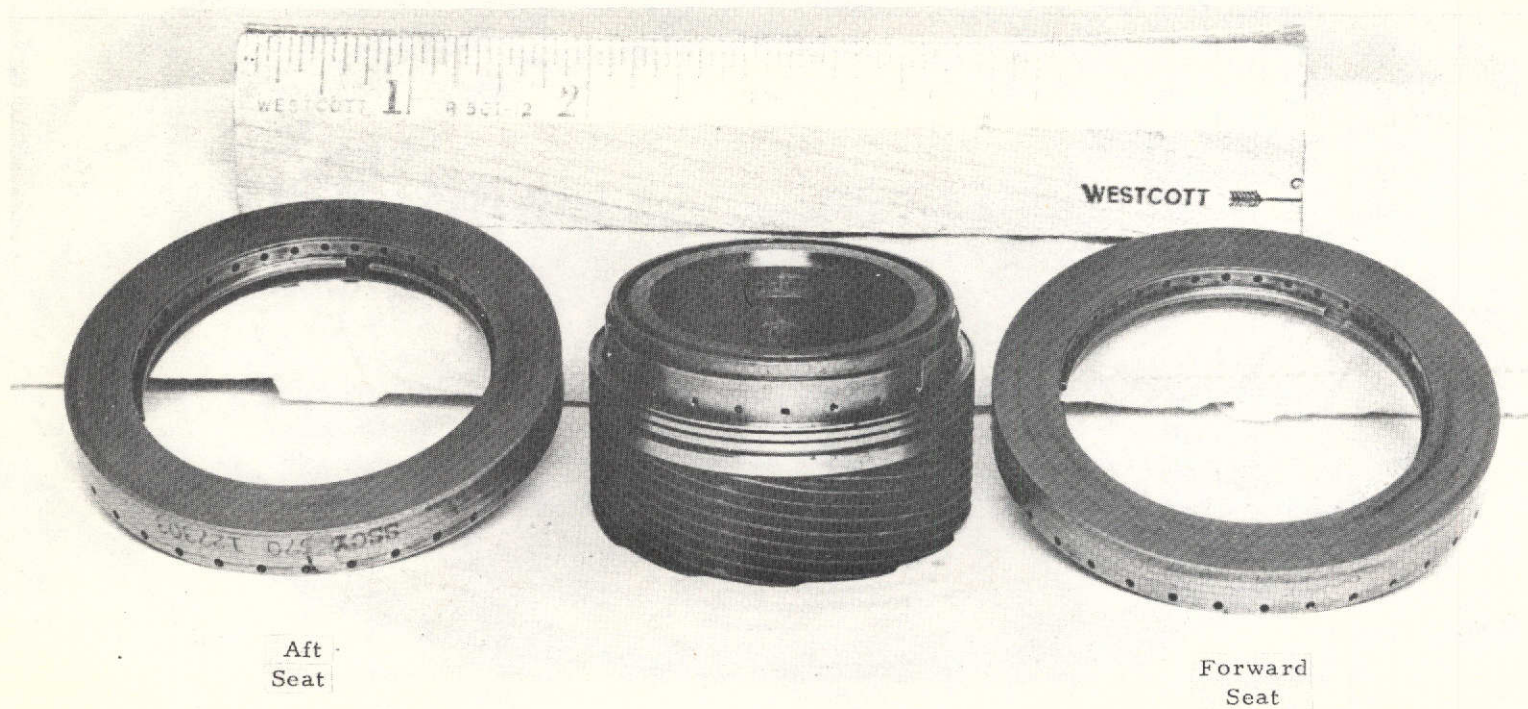


Figure 33. Seal Seats and Aft Rotating Windback After Sand and Dust Test IV.

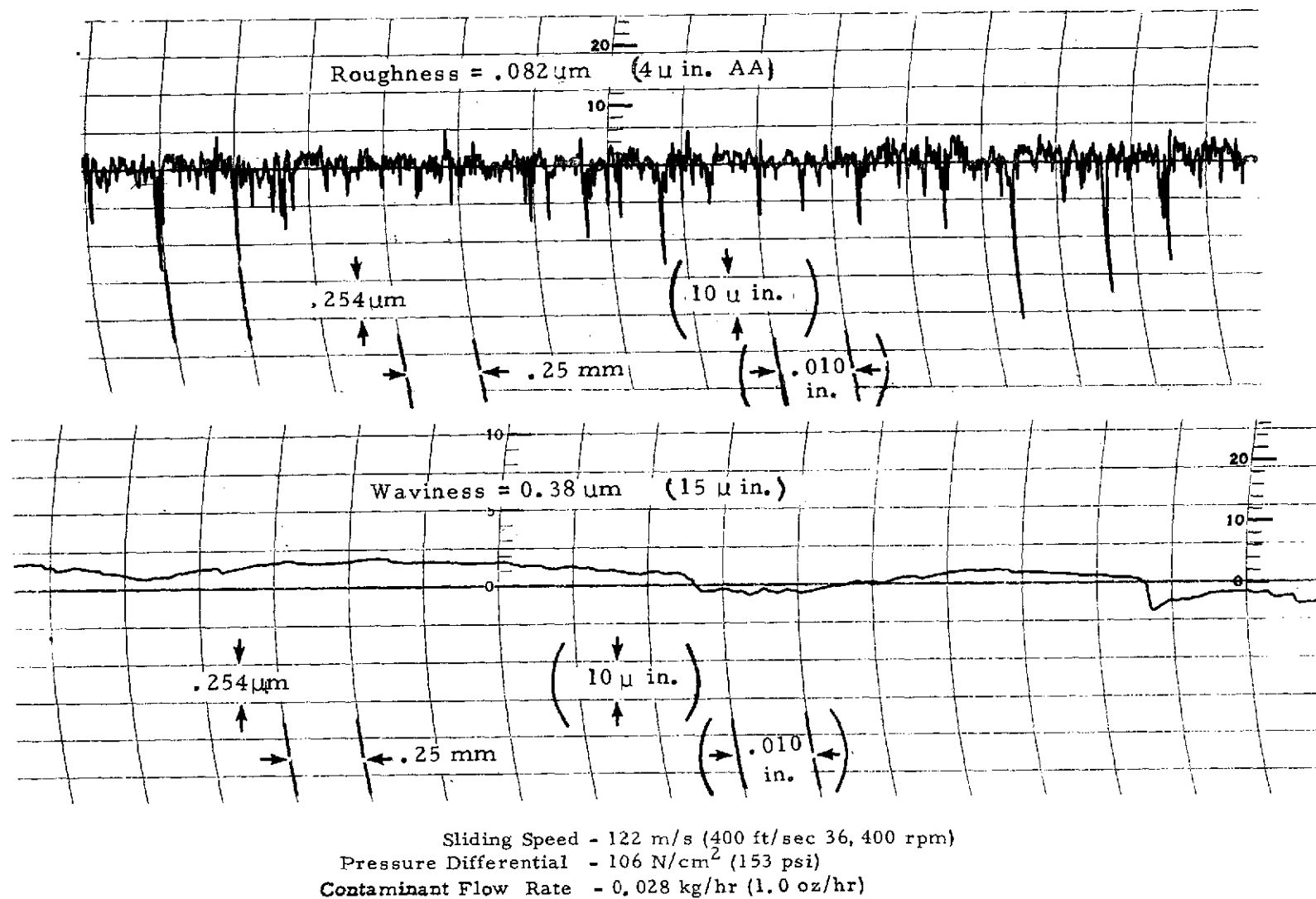
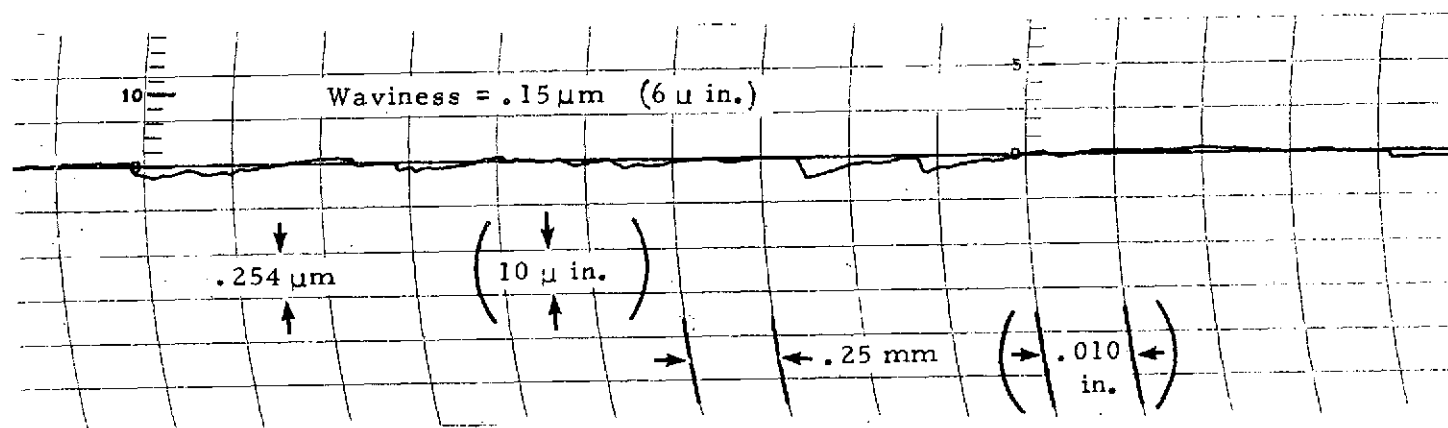
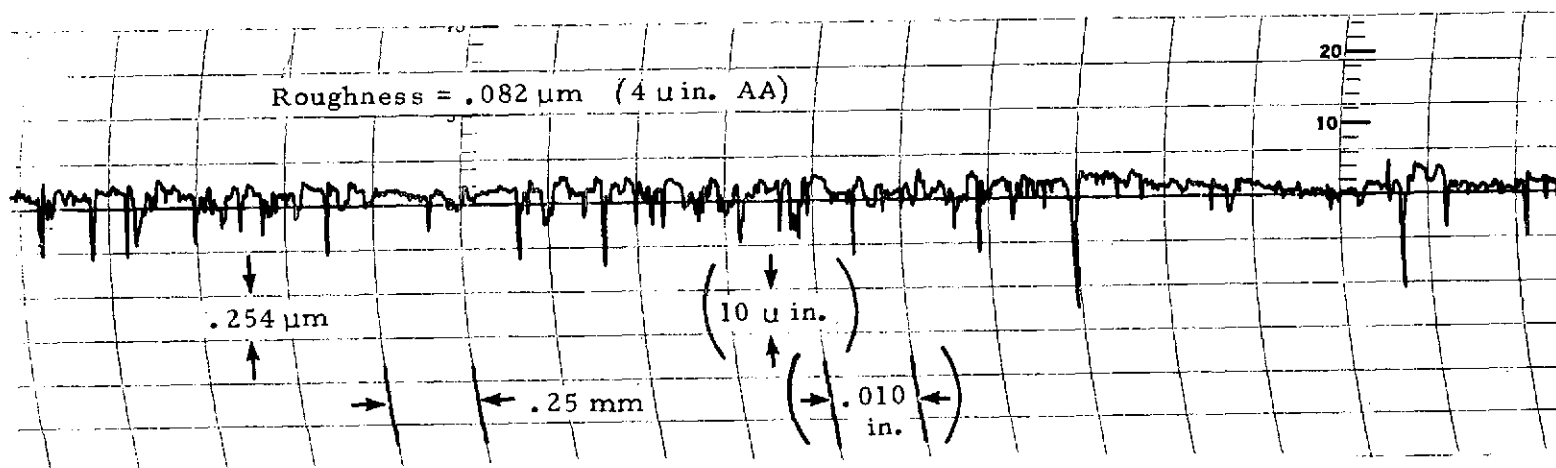
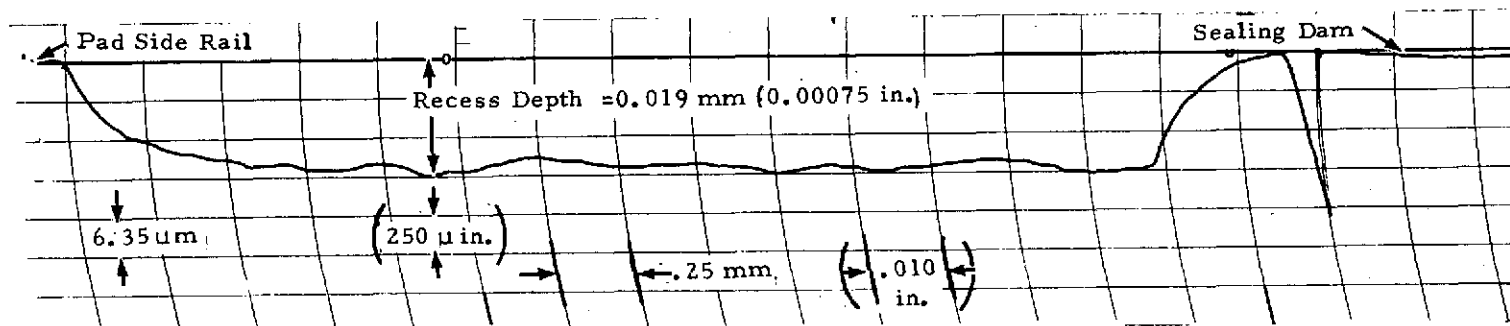


Figure 34. Forward Seal Seat Surface Texture After Sand and Dust Test IV -
 Taken in a Radial Direction on the Seat Face Across the Running Track.

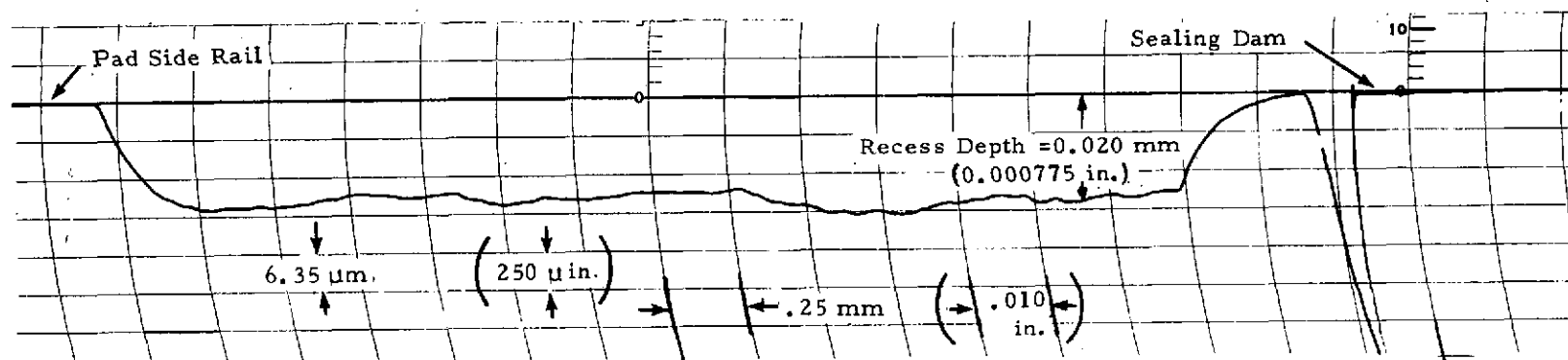


Sliding Speed - 122 m/s (400 ft/sec 36,400 rpm)
 Pressure Differential - 106 N/cm^2 (153 psi)
 Contaminant Flow Rate - 0.028 kg/hr (1.0 oz/hr)

Figure 35. Aft Seal Seat Surface Texture After Sand and Dust Test IV. - Trace Taken in a Radial Direction on the Seat Face Across the Running Track.



Forward Seal



Aft Seal

Sliding Speed - 122 m/s (400 ft/sec 36,400 rpm)
 Pressure Differential - 106 N/cm² (153 psi)
 Contaminant Flow Rate - 0.028 kg/hr (1.0 oz/hr)

Figure 36. Typical Lift Pad Traces of Forward and Aft Seal After Sand and Dust Test IV.

Discussion

The amount of sand ingested by the rig in test I, 0.028 kg/hr (1 oz/hr) was far greater than would be seen in a practical application. Reference 9 suggests 0.0035 kg/hr (0.125 oz/hr) as sufficient sand and dust to cause measurable seal wear in a 10-hour period. Test II and III with 0.0028 and 0.0084 kg/hr (.1 and .3 oz/hr) were conducted for 6.5 hours and 10 hours with negligible carbon wear.

In order to determine the influence of the change in direction of thrust of the rotating windback, test IV was conducted with the same excessive sand and dust rate as test I; 0.028 kg/hr (1 oz/hr). Seal operation was stable for 10 hours with carbon wear less than 0.0025 mm (0.0001 in.) indicating the second windback configuration was more effective than that used in test I.

CONCLUSIONS AND RECOMMENDATIONS

The self-acting face seal demonstrated a high speed and air pressure capability in 500 hours of endurance testing at sliding speeds of 183 m/s (600 ft/sec, 54,600 rpm) and air pressure differential of 137 N/cm² (198.7 psi). These conditions are more severe than experienced in present engines and are beyond the capacity of conventional seal configurations.

A redesign of the self-acting face seal is required to overcome difficulties related to thermal distortion of the face plate leading to contact of the sealing surfaces during operation, excessive heat generation, and wear.

Operation with excessive seal seat axial runout did not cause seal component distress; however, airflow increased.

The self-acting face seal showed a tolerance for operation in a severe sand and dust environment. Carbon wear was minor, and operation was stable.

Endurance testing, runout, and sand and dust operation have demonstrated the feasibility of the self-acting face seal for operation in advanced gas turbine engine main shaft seal applications.

REFERENCES

1. Lynwander, P. : "Development of Helicopter Engine Seals" Avco Lycoming Report LYC 73-48, NASA CR-13467, 1973.
2. Ludwig, L. P., and Johnson, R. L. : "Design Study of Shaft Face Seal with Self-Acting Lift Augmentation. III - Mechanical Components, "NASA TN D-6164, 1971.
3. Ludwig, L. P., Zuk, J., and Johnson, R. L. : "Design Study of Shaft Face Seal with Self-Acting Lift Augmentation. IV - Force Balance, " NASA TN D-6568, 1972.
4. Zuk, J., Ludwig, P., and Johnson, R. L. : "Quasi-One-Dimensional Compressible Flow Across Face Seals and Narrow Slots. I - Analysis, "NASA TN D-6668, 1972.
5. Zuk, J., and Ludwig, L. P. : "Investigation of Isothermal, Compressible Flow Across a Rotating Sealing Dam. I - Analysis, "NASA TN D-5344, 1969.
6. Zuk, J., and Smith, P. J. : "Computer Program for Viscous Isothermal Compressible Flow Across a Sealing Dam with Small Tilt Angle, " NASA TN D-5373, 1969.
7. Zuk, J., Ludwig, L. P., and Johnson, R. L. : "Design Study of Shaft Face Seal with Self-Acting Lift Augmentation. I - Self-Acting Pad Geometry, " NASA TN D-5744, 1970.
8. Colsher, R., and Shapiro, W. : "Steady State and Dynamic Performance of Gas-Lubricated Seals, "NASA CR-121093, 1972.
9. Dobek, L. J. : "Development of Mainshaft Seals for Advanced Air Breathing Propulsion Systems, " Pratt and Whitney Aircraft Rep. PWA TM-4683, NASA CR-121177, 1973.

DISTRIBUTION

NASA Headquarters Washington, D. C. 20546 Attn: N. F. Rekos (RLC)	1	Department of the Navy Bureau of Ships Washington, D. C. 20525 Attn: Harry King, Code 634A	1
J. Maltz (RWM)	1		
D. Miller (RLC)	1		
NASA Lewis Research Center 21000 Brookpark Road Cleveland, Ohio 44135 Attn: A. Ginsburg, MS 5-3	1	Department of Navy Naval Air Systems Command AIR-330 Washington, D. C. 20360	1
R. L. Johnson, MS 23-2	1		
L. P. Ludwig, MS 23-2	20	U. S. Navy Marine Engineering Laboratory Friction and Wear Division Annapolis, Maryland 21490 Attn: R. B. Snapp	1
M. A. Swikert, MS 23-2	1		
L. W. Schopen, MS 500-206	1		
Report Control Office, MS 5-5	1		
Library, MS 60-3	2	Department of the Navy Office of Naval Research Code 411 Arlington, Virginia 22217 Attn: Lt. R. Miller	
Technology Utilization Office, MS 3-19	1		
W. L. Stewart MS 3-5	1		
C. H. Winzig MS 5-3	1		
N. T. Musial, MS 500-113	1	Department of the Army U. S. Army Aviation Materials Labs Fort Eustis, Virginia 23604 Attn: John W. White, Chief, Propulsion Division	1
W. F. Hady, MS 23-2	1	R. Givens	1
Dr. J. Zuk, MS 23-2	1		
NASA-Scientific and Technical Information Facility P. O. Box 33 College Park, Maryland 20740 Attn: NASA Representative	2		
NASA-Langley Research Center Langley Station Hampton, Virginia 23365 Attn: Mark R. Nichols	1	U. S. Army Ordnance Commander Rock Island Arsenal Rock Island, Illinois 61201 Attn: SARRI - LR - M	1
NASA-Manned Spacecraft Center Houston, Texas 77058 Attn: C. D. Haines	1	AMMRC Watertown, Massachusetts 02172 Attn: Dr. R. Singler	1
United States Air Force Wright-Patterson Air Force Base AF Systems Command USAF Wright-Patterson AFB, Ohio 45433 Attn: AFAPL (APDL), K. L. Berkey	1	AVCOM AMSAVEGTT Mart Building 405 South 12th Street St. Louis, Missouri 63166 Attn: E. England	1
AFAPL (AFTC), C. Simpson	1		
APTP, I. J. Gershon	1		
MANE, R. Headrick	1		
MANE, P. House	1	Commander U. S. Aviation Systems Command P. O. Box 209 St. Louis, Missouri 63166 Attn: J. Means SAVDL - SR	
TBC, C. Elrod	1		
APFL/SFL, Howard Jones	1		
U. S. Naval Research Laboratory Washington, D. C. 20390 Attn: Charles Murphy	1	Aerojet-General Corporation 20545 Center Ridge Road Cleveland, Ohio 44110 Attn: D. B. Rake	1
Department of the Navy Bureau of Naval Weapons Washington, D. C. 20013 Attn: A. D. Nehman, RAAE-3 C. C. Singletorry, RAPP-4	1	AiResearch Manufacturing Corporation 402 S. 36th Street Phoenix, Arizona 85034 Attn: F. Blake Wallace	2
U. S. Army Air Mobility R&D Lab SAVDL-LE-PP Lewis Directorate (MS 500-317) 21000 Brookpark Road Cleveland, Ohio 44135 Attn: Lt. Col. G. Weden John Acurio	1	Avco Corporation Lycoming Division 550 South Main Street Stratford, Connecticut 06497 Attn: R. Cuny P. Lynwander	1
	1		1

Battelle Memorial Institute 505 King Avenue Columbus, Ohio 43201 Attn: C. M. Allen	1	Durametallic Corporation Kalamazoo, Michigan 49001 Attn: H. Hummer	1
Bendix Corporation Fisher Building Detroit, Michigan 48202 Attn: R. H. Isaacs	1	Fairchild Hiller Corporation Republic Aviation Division Farmingdale, L.I., New York 11735 Attn: C. Collis	1
B. F. Goodrich Company Aerospace & Defense Products Division Troy, Ohio 45373 Attn: L. S. Blalkowski	1	Franklin Institute Laboratories 20th and Parkway Philadelphia, Pennsylvania 19103 Attn: W. Shapiro	2
Boeing Aircraft Company P. O. Box 3707 Seattle, Washington 98124 Attn: W. S. Lambert, 2-1100 W. C. Nelson	1	Garrett Corporation AirResearch Manufacturing Division 9851-9951 Sepulveda Boulevard Los Angeles, California 90009 Attn: A. Silver	1
The Boeing Company Vertol Division P. O. Box 16859 Philadelphia, Pennsylvania 19142 Attn: A. J. Lemanski, MS P-32-09	1	General Dynamics Corporation 1025 Connecticut Avenue, N. W. Washington, D. C. 20036 Attn: G. J. Vila	1
Borg-Warner Corporation Roy C. Ingersoll Research Center Wolf and Algonquin Roads Des Plaines, Illinois 60018	1	General Electric Company Advanced Engine & Technology Department Cincinnati, Ohio 45215 Attn: L. B. Venable	1
Chicago Rawhide Manufacturing Company 1311 Elston Avenue Chicago, Illinois 60622 Attn: R. Blair	1	N. Pope	1
Clevite Corporation Cleveland Graphite Bronze Division 17000 St. Clair Avenue Cleveland, Ohio 44110 Attn: J. Ross	1	W. McCarty	1
Cooper Bessemer Mt. Vernon, Ohio 43050 Attn: K. Smith	1	I. E. Sumey	1
Crane Packing Company 6400 W. Oakton Street Morton Grove, Illinois 60053 Attn: Harry Tankus	1	T. Russell	1
Defense Ceramics Information Center Battelle Memorial Institute Columbus Labs, Room 11-9021 505 King Avenue Columbus, Ohio 43201	1	J. Clark	1
Dresser Industries Dresser Clark Division P. O. Box 560 Olean, New York 14780 Attn: J. W. Kirkpatrick E. Tanzberger	1	General Motors Corporation Allison Division Plant #3, Department 7339 Indianapolis, Indiana 46206 Attn: E. M. Deckman	1
	1	Gould Information Center 540 E-150th Street Cleveland, Ohio 44108 Attn: L. A. Noble	1
		IIT Research Foundation 10 West 35 Street Chicago, Illinois 60616 Attn: Dr. Strohmeir M. A. Schwartz	1

Koppers Company, Inc. Metal Products Division Piston Ring and Seal Department P.O. Box 626 Baltimore, Maryland 21203 Attn: E. Taschenburg J. Heck	1 1 1	Pesco Products Division Borg-Warner Corporation 24700 N. Miles Bedford, Ohio 44146 Attn: W. J. Cieslik	1
Lockheed Aircraft Company 118 West First Street Dayton, Ohio 45402 Attn: R. R. Witte	1	Poco Graphite, Incorporated P.O. Box 1524 Garland, Texas 75040 Attn: Dr. R. F. Wehrmann	1
Los Alamos Scientific Laboratory University of California Los Alamos, New Mexico Attn: M. C. Smith	1	Pure Carbon Company, Inc. 441 Hall Avenue St. Marys, Pennsylvania 15857 Attn: Dr. R. R. Paxton J. Sherlock	1 1
Martin Marietta Corporation 1700 Needmoor Road Dayton, Ohio 45414 Attn: Z. G. Horvath	1	Rexnord-Seal Division 1311 Elston Avenue Chicago, Illinois 60622 Attn: John Harrop	1
McDonnell Douglas Corporation 333 West First Street Dayton, Ohio 45402 Attn: R. G. Donmoyer	1	Sealol, Incorporated P.O. Box 2158 Providence, Rhode Island 02905 Attn: Justus Stevens E. Moran	1 1
Mechanical Technology, Inc. 968 Albany-Shaker Road Latham, New York 12110 Attn: Donald F. Wilcock	1	Sikorsky Aircraft North Main Street Stratford, Connecticut 06497 Attn: Carl Keller	1
Midwest Research Institute 425 Volker Boulevard Kansas City, Missouri 64110 Attn: V. Hopkins	1	SKF Industries, Incorporated 1100 First Avenue King of Prussia, Pennsylvania 19406 Attn: L. B. Sibley	1
NASA Scientific Technical Information Facility Acquisitions Branch P.O. Box 33 College Park, Maryland 20740	10	Southwest Research Institute P.O. Drawer 28510 San Antonio, Texas 78228 Attn: P. M. Ku	1
North American Rockwell Corporation 5100 West 164 Street Cleveland, Ohio 44125 Attn: George Bremer	1	Space Craft, Incorporated 5670 Markdale Drive Dayton, Ohio 45459 Attn: J. W. Sharp	1
North American Rockwell Corporation Rocketdyne Division 6633 Canoga Avenue Canoga Park, California 91304 Attn: R. E. Burcham	1	St. Marys Carbon Company 1939 State Road St. Marys, Pennsylvania 15857 Attn: J. E. Lanzel	1
Northrop Corporation 379 West First Street Dayton, Ohio 45402 Attn: Dr. W. A. Martin	1	Stackpole Carbon Company St. Marys, Pennsylvania 15857 Attn: Dr. E. I. Shobert	1
		Stanford Research Institute 333 Ravenwood Avenue Menlo Park, California 94025 Attn: R. C. Fey	1

Stein Seal Company
20th Street and Indiana Avenue
Philadelphia, Pennsylvania 19132

Attn: Dr. P. C. Stein 1
E. Goldring 1

Ultra Carbon Corporation
1300 N. Madison Avenue
Bay City, Michigan 48706
Attn: Del Hughes 1

Union Carbide
Carbon Products Division
P.O. Box 6116
Cleveland, Ohio 44101
Attn: N. Fectter 1

United Aircraft Corporation
Pratt & Whitney Aircraft Division
Engineering Building EB2B-2
East Hartford, Connecticut 06108
Attn: R. Shevchenko 3
V. Povinelli 1
P. Brown 1

Wickes Engineered Materials
1621 Holland
Saginaw, Michigan
Attn: Paul Dahlenberg 1

The University of Tennessee
Department of Mechanical and Aerospace
Engineering
Knoxville, Tennessee 37916
Attn: Professor W. K. Stair 1

Westinghouse Electric Corporation
5100 W. 164 Street
Cleveland, Ohio 44142
Attn: Lynn Powers 1

Williams Research Corporation
2280 W. Maple Road
P.O. Box 95
Walled Lake, Michigan 48088
Attn: K. J. Bremner 1